Nano Research

Open Access

Review Article

Functionalized protein nanopores: Strategies and applications

Ke Sun[1], Mengze Wu[1], Yu Xin[1], Yue Li[1], Minghan Li[1], Jinna Wang[3], Yuan Ju[2] ✉, Shengli Zhang[3] ✉, and Jia Geng[1,4] ✉

[1] *Department of Laboratory Medicine, State Key Laboratory of Biotherapy and Cancer Center, West China Hospital, Sichuan University and Collaborative Innovation Center, Chengdu 610041, China*
[2] *Sichuan University Library, Sichuan University, Chengdu 610041, China*
[3] *Department of Food Science and Engineering, School of Agriculture and Biology, Shanghai Jiao Tong University, Shanghai 200240, China*
[4] *Tianfu Jincheng Laboratory, City of Future Medicine, Chengdu 641400, China*

Cite this article: *Nano Research*, **2026**, *19*, 94908343. https://doi.org/10.26599/NR.2026.94908343

ABSTRACT: Over the past years, significant progresses have been made in the field of nanopores, particularly in single-molecule analysis, sequencing, and diagnostic applications, certainly underscoring the versatility of stochastic nanopore sensing. The subsequent advances in functionalizing protein nanopores with tailored properties or reactive handles have greatly expanded their detection capabilities, where customized computational design shows promise in driving nanopore functionalization and applications toward unprecedented flexibility. In this review, we provide a comprehensive perspective of the various engineering strategies employed in protein nanopores and the roles of functionalized nanopore in single-molecule sensing and sequencing. Additionally, we elucidate the interplay between functionalization strategies and their intended applications, highlighting promising implementation scenarios. We believe that the ongoing advancements in functionalization technologies will promote innovations in de novo pore design and propel nanopore protein sequencing.

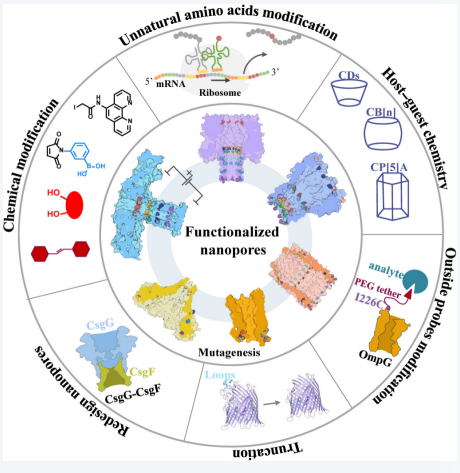

KEYWORDS: nanopore sensing, functionalized protein nanopore, single-molecule analysis, engineering strategies, applications

1 Introduction

Nanopore technology, inspired by the Coulter counter, has evolved over three decades, transitioning from its origins as a blueprint for ultra-sensitive DNA sequencing to the widespread commercialization of nanopore sequencing devices by Oxford Nanopore Technologies [1–5]. Over this period, the field has advanced at a pace exceeding Moore's Law, and earned recognition from *Nature Methods* as "Method of the Year" in 2023 for its ability to produce long continuous reads spanning tens to hundreds of kilobases [6]. In a typical nanopore stochastic sensing experiment, an individual analyte enters the nanopore under an applied bias voltage, altering the flow of ions through the pore and being reflected in a time-dependent ionic current recording [7–9]. Through the analysis of current fluctuations, including blockade amplitude, deviation, duration, and frequency, nanopores have been effectively employed for stochastic sensing and the detailed characterization of DNA [10, 11], RNA [12, 13], peptides [14, 15], proteins [16, 17], small molecules [18, 19], and metabolites [20, 21] at the single-molecule level.

Nanopore stochastic sensing primarily relies on the pore diameter and the confined functionalized surface of the cavity [22–25]. Protein nanopores are formed by the self-assembly of multiple subunits in lipid bilayers or synthetic block copolymer membranes [26–29]. They possess atomically precise in nano- or sub-nanometer dimensions, providing the ability to recognize biomolecules with comparable size [30]. In contrast, solid-state nanopores are often crafted with flexible diameters ranging up to hundreds of nanometers in materials such as silicon oxide films, glass capillaries or other substrates [31]. While this scale is well-suited for sensing biomacromolecules, it is significantly larger than most of biomolecules, which often necessitate pores at the lower end of this range. Solid-state nanopores tend to be much more

Received: October 30, 2025; **Revised:** December 12, 2025
Accepted: December 14, 2025

✉Address correspondence to Jia Geng, geng.jia@scu.edu.cn; Shengli Zhang, zhangshengli@sjtu.edu.cn; Yuan Ju, yuan.ju@scu.edu.cn

mechanically, thermally and chemically stable than their biological counterparts [31]. However, the top-down approaches used in their fabrication, such as laser- or electron-beam etching, limit atomic-scale structural control. This limited precision, coupled with the relatively inert substrates that often lack the maneuverability for further customized modification, leads to restricted spatial and temporal resolution [32–34]. Conversely, while assembled protein nanopores typically require a carefully controlled environment and strict conditions for operation, they feature more precise dimensions defined by their protein sequences, offering substantial opportunities for extensive modification through genetic or chemical approaches [35–37].

For protein nanopores, in addition to the expansion of applications driven by the discovery of innovative pores, the significant breakthroughs in stochastic sensing over the past few decades have been primarily tied to the modification, reconstruction, and even de novo design of protein pores [38, 39]. As the dominant application in nanopore technology, stochastic sensing demands a delicate equilibrium between high-frequency single-molecule capture and prolonged translocation through the pore constriction [40, 41]. To achieve this critical balance for the specific applications, nanopores have been undergone different evolutionary and modification strategies to optimize performance [42]. These modifications typically involve site-directed mutagenesis, the incorporation of unnatural amino acids, etc. These approaches enable targeted enhancements, such as tuning cavity electrostatics to modulate electroosmotic effects and improve capture efficiency and temporal resolution [42–45]. Additionally, by introducing biomacromolecules such as nucleic acid aptamers or immune molecules at the nanopore entrance, the capture efficiency can be further improved by the "grasping" effect of these functional groups [46–48]. This allows the nanopore to controllably capture, identify, and transport a wide variety of molecules and ions from the bulk solution. Beyond molecular detection, nanopores are also employed to directly measure the structural and chemical properties of analytes, enabling the identification of isomers and track chemical transformations at the single-molecule level [17, 49–52]. Achieving such precision typically requires sophisticated modifications to the nanopore, particularly within the sensing region. Active residues on the surface of the nanopore cavity could be spatially engineered and aligned within a protein nanopore through site-directed mutations or chemical modifications, creating a confined chemical microenvironment that facilitates site-selective or regio-selective covalent chemistry [53, 54]. Another common approach involves metal chelation [55], often based on click chemistry [56], or host-guest interactions [57, 58], to introduce specific recognition capabilities into nanopores. These innovations have made notable achievements in the development of single-molecule protein sequencing methods, which enable the precise identification of amino acids [59–61]. Another promising avenue for single-molecule protein sequencing is the development of nanopore-based molecular machine, which typically relies on the precise design and synergistic systems that combine nanopores with enzymes to facilitate controlled analyte translocation and sequencing [60, 62].

Herein, we present a comprehensive overview of recent advances in protein nanopore modification, examining emerging strategies for optimizing nanopore functionality. Although previous reviews have summarized some engineering approaches and corresponding sensing applications [34, 63], this review systematically outlines evolving modification strategies for protein nanopores, organizing them from an application-oriented perspective. We aim to elucidate the underlying design principles and to provide conceptual guidance for future innovation in nanopore sensing. In addition, we further discuss persistent challenges and potential opportunities to shape the future of protein nanopores.

2 Site-directed mutagenesis of protein nanopores

Site-directed mutagenesis has extensively employed for the modification of protein nanopores, as they can modulate geometry and charge distribution through residue substitution, hence expanding sensing ranges and improving sensitivities of nanopores. Here, we systematically summarized prevalent strategies for mutagenesis, and delineated the mutation sites as well as the sensing application of protein nanopores (Figs. 1 and 2).

2.1 Mutations for enhancing resolution of sensing

The manipulation of electrostatic properties within protein nanopores is a pivotal strategy to enhance the resolution, often achieved through targeted mutations at the pore-sensing region. For instance, the incorporation of positively charged residues such as arginine (R) and lysine (K) at M113 and/or T145 sites within the α-hemolysin (α-HL) nanopore significantly strengthen electrostatic interactions with negatively charged analytes, including phosphate esters, acetamido and carboxyl groups [64, 65]. These mutations cause prolonged blockage durations and improved temporal resolution, hence broadening the sensing applications of α-HL nanopore to detect anionic peptides [66], 1,4,5-trisphosphate [65, 67], inositol hexakis-phosphate [68], and metal ions [64]. Additional advancements include mapping acetylamino and carboxyl groups on glycans [69, 70], characterizing long ssRNA [71], and detecting DNA at alkaline pH [72]. Similarly, the T232K mutation in aerolysin (AeL) nanopore creates an electrostatic trap that enhances electrostatic interaction with peptides, thus prolonging translocations time and enabling the detection of post-translational modifications (PTMs) [73–75]. The AeL (T240R) nanopore detected neutral glycan with a R-binaphthyl tag, benefiting from the enhanced cation-π interaction between the R-binaphthyl tag and mutant R240 [76]. Furthermore, introducing R near the constriction of MspA nanopore (L88R) has been shown to increase the dwell time of homopolymers ssDNA [77]. Negative charged mutants, like the α-HL (M113E), identified cationic peptide through similar enhancement of electrostatic interaction [66].

Introduction of neutral residues is strategically employed to reduce or eliminate electrostatic barriers. A notable example is demonstrated by the engineering of M1MspA and M2MspA. The acidic residues D90, D91, and D93 at the constriction were substituted with neutral asparagine residues (D90N/D91N/D93N), resulting in high signal-to-noise ratio (SNR) and single nucleotide resolution for ssDNA analysis [78, 79]. The M2MspA was subsequently integrated with motor protein such as DNA polymerase phi29, the helicase Hel308 [80, 81], helicase MTA [82], helicase PcrA [83], and SARS-CoV-2 NSP13 helicase [84] to modulate the velocity of DNA translocation, thus developing the single-molecule picometer-resolution nanopore tweezers (SPRNT) technique [85]. This approach enabled nanopore-based DNA sequencing and high-precision detection of mutagenic DNA lesions, including O^6-carboxymethyl guanine [86], 5-

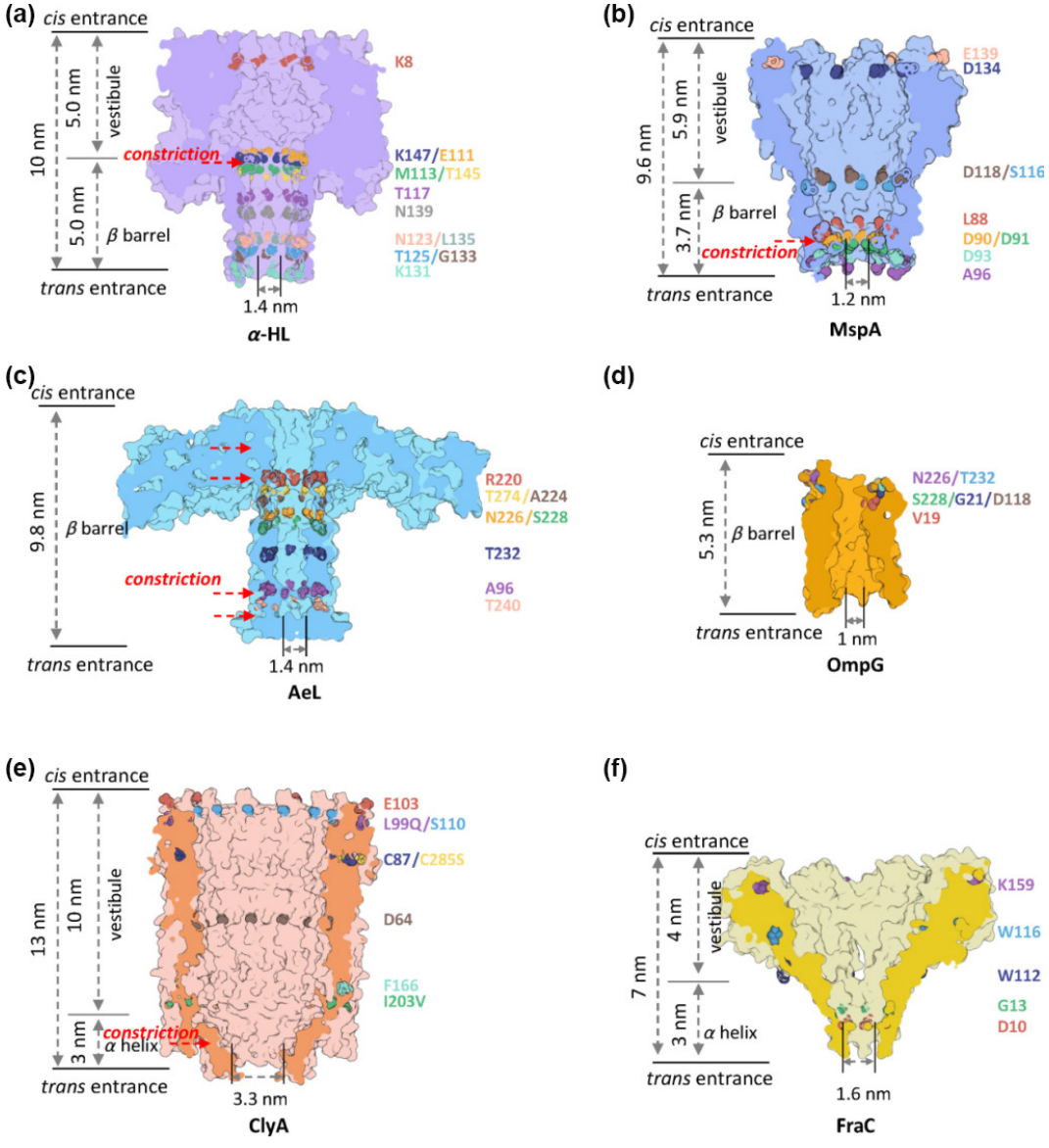

Figure 1 Structure and mutation sites of protein nanopores. (a) α-HL: Staphylococcal α-hemolysin (Protein Data Bank Identifier (PDB ID): 3ANZ); (b) MspA: *Mycobacterium smegmatis* porin A (PDB ID: 1UUN); (c) AeL: *Aeromonas hydrophila* aerolysin (PDB ID: 5JZT); (d) OmpG: *Escherichia coli* outer membrane protein G (PDB ID: 2IWV); (e) ClyA: *Salmonella enterica* cytolysin A (PDB ID: 2WCD); (f) FraC: *Actinia fragacea* fragaceatoxin C (PDB ID: 4TSY).

methylcytosine, and 5-hydroxymethylcytosine [87], and even unnatural DNA nucleotides [81, 88]. Furthermore, the SPRNT has been extended to peptide sequencing through DNA-peptide conjugates [80, 82, 89]. Besides, M2MspA exhibits considerable potential for detecting peptides [90], analyzing protein structures [91], monitoring conformational change in nucleic acids [92], and identifying proteins with different isoelectric points [93]. Another example is the AeL (K238Q) nanopore, which also provides high resolution for sensing nucleotides [94, 95], phosphorylation [11, 96], and transient conformations of flavin adenine dinucleotide [97]. The ultra-high resolution for nucleic acids enables this mutant pore to precisely probe the reaction kinetics of nucleic acid–related enzymes at the single-molecule level. For example, the AeL (K238Q) nanopore has revealed the temporal dynamics and heterogeneous cleavage, and release pathways of ssDNA by Exo I [98].

The strategies to enhance sensing resolution also involves introducing aromatic amino acids to enable π–π stacking interactions, increasing steric hindrance with bulky residues, and incorporating hydrophobic residues to promote hydrophobic interactions. For instance, the α-HL (M113F) nanopore exhibits prolonged event residence time for peptides compared to the wild-type (WT) pore [99]. This enhancement enables the pore to monitor uranyl ions [100], HIV-1 protease and trypsin [101, 102]. Similar improvements could be observed in FraC (G13F) nanopore, which showed increased peptide capture frequency and dwell time, and it is capable of identifying individual proteins through measuring protein fingerprinting and recognizing glycosylated peptides [103, 104]. However, it is crucial to note that the enhancement depends on the specific mutation site, and the precise orientation and angle of the residue within the nanopore lumen. Sometimes, non-aromatic amino acids with bulky side chain, such as glutamine (Q), have been introduced at constriction to improve spatial resolution. For example, the AeL (N226Q) nanopore formed

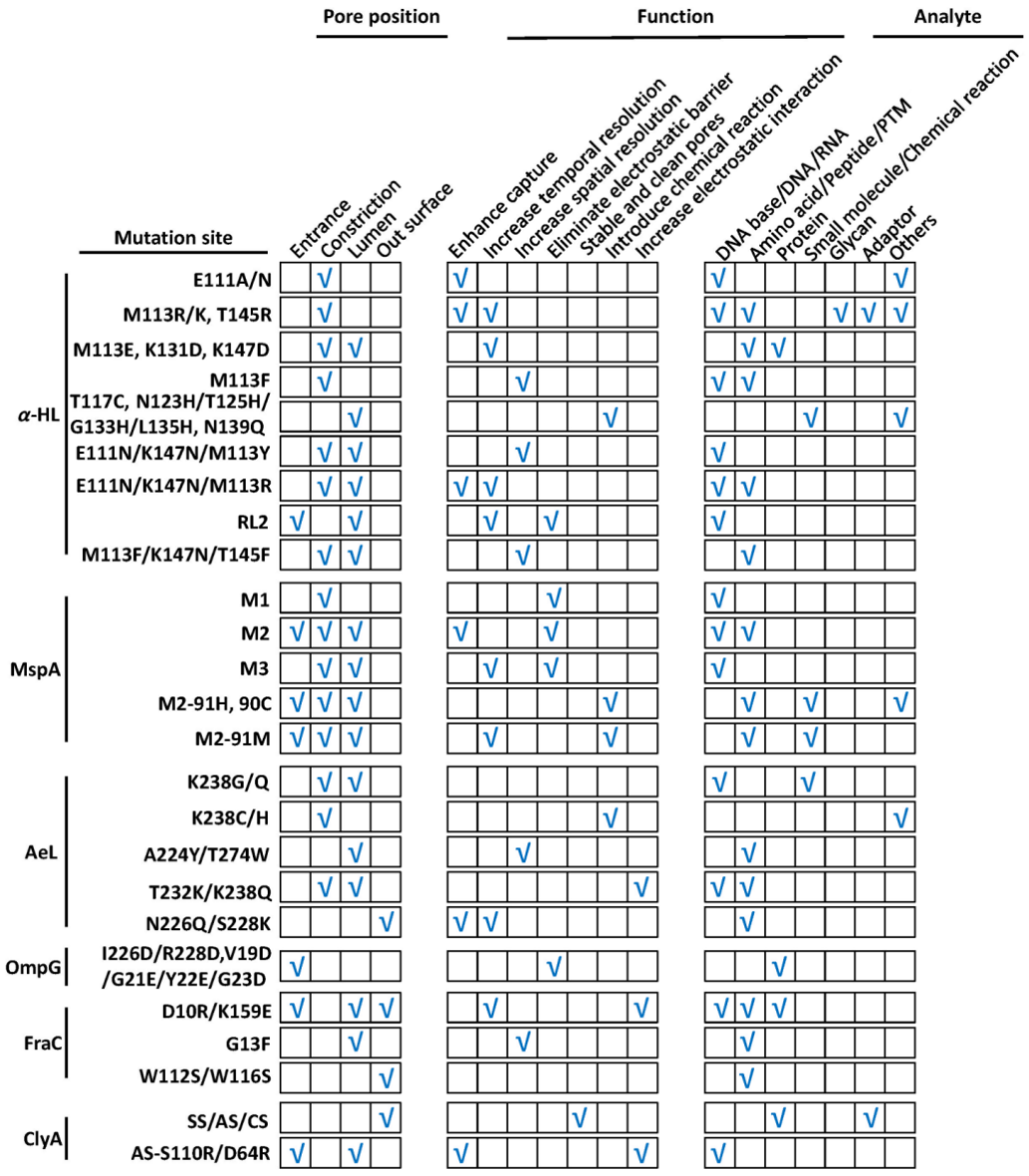

Figure 2 Characteristics of protein nanopore mutants. Pore positions, functions, and analytes of the different mutants for protein nanopores. RL2 of α-HL: α-HL (K8A/V124L/G130S/N139Q/I142L), M1 of MspA: M1MspA (D90N/D91N/D93N), M2 of MspA: M2MspA (D90N/D91N/D93N /D118R/D134R/E139K), M3 of MspA: M3MspA (L88R/D90N/D91N/D93N/A96R/S116R), SS of ClyA: ClyA-SS (C87S/C285S), AS of ClyA: ClyA-AS (C87A/L99Q/E103G/F166Y/I203V/C285S/K294R/H307Y), CS of ClyA: ClyA-CS (L99Q/E103G/F166Y/C285S/K294R).

a new narrower constriction (0.8–1.2 nm), thereby prolonging the dwell times of peptides [105]. Conversely, reducing steric hindrance within the lumen sometimes also enhanced macromolecular recognition. For instance, the engineered AeL (K238A) with a shorter side chain showed improved resolution for sequence-defined poly(phosphodiester)s [106, 107]. Additionally, recent studies have highlighted that the interactions of hydrophobic residues within the nanopore sensing region exert a pronounced enhancing effect, particularly when using the AeL (A224Y/T274W) and CytK (Q5Y/S149I) nanopores to detect peptides and unfolded proteins [45, 108].

Single-point mutation exerts limited influences on improving the performance of nanopores. The combination of multiple mutations might result in a significant enhancement of nanopore functionality. For instance, the K131D/K147D mutation in α-HL nanopore produces electrostatic traps near the entrances and exits, which provide controlled translocation and extended duration time of single polypeptides and protein [109–111]. Moreover, the α-HL (E111N/K147N/M113R, NN-113R) nanopore confers anion selectivity, and it enables to directly detect PTMs within long polypeptides [112, 113] and recognize the four DNA bases at high pH [114]. The synergistic effects of charged and aromatic amino acid mutations enhance the spatial and temporal resolution. For instance, the α-HL (E111N/K147N/M113Y, NNY) nanopore improves recognition properties and has been used to identify epigenetic DNA modifications [115], recognize RNA base [116], and sequence DNA [117]. Additionally, the double aromatic residues mutant M113F/K147N/T145F (2FN) demonstrates high selectivity in distinguishing short peptides [99]. The combination of charged amino acids mutations and steric mutations, like AeL (T232K/K238Q), has been utilized to sense DNA [118, 119] and map the adjacent phosphorylation sites of Tau peptide with greater

temporal and spatial resolution [118].

The strategy of introducing reactive residues at specific sites enables the development of innovative sensing approaches through chemical interactions. For example, the introduction of cysteine (C) at the T117 site of α-HL nanopore were developed to rapidly detect nitrogen mustards through a coupling reaction with thiol group [120]. Importantly, the engineered hetero-α-HL nanopore has demonstrated the potential to monitor site-selective thiol–disulfide interchange reactions with atomic precision [54, 121] and has been employed as a proof-of-concept for enzymeless nanopore DNA sequencing [25, 53]. This strategy could also be observed in other β-barrel nanopore, such as AeL. Given its extended lumen, numerous tunable pore-facing residues, and well-defined confined space within the pore, AeL is particularly suited for monitoring chemical kinetics. The AeL (K238C) was designed to monitor the chemical reaction of disulfide bonds [122, 123], and to enable real-time visualization of the dynamic thiol substitute reactions [124]. Moreover, this cysteine mutant of AeL can also serve as an effective nanoreactor to monitor the kinetics of bond-forming processes [125]. Importantly, the cysteine residues within the sensing region have facilitated chemical modifications via Michael addition reactions to further extend the sensing application of nanopore (details were in Section 5). Additionally, the histidine (H) and methionine (M) have been introduced to AeL and M2MspA nanopore. The AeL (K238H) nanopore was utilized to measure the coordination reactions between histidine and Au(III) [126], and the MspA-91M mutants detect Dichloroaurate(I) and tetrachloroaurate(III) with methionine through metal ions chelation [127, 128]. Notably, the MspA-91H was able to precisely identify and quantify all 20 amino acids using copper(II) chelation [55]. These advances provide a proof-of-concept for nanopore-based protein sequencing.

2.2 Mutations for enhancing capturing frequency

The successive capture of analytes is critical for nanopore sensing, as the abundance of the statistical events directly influences the accuracy of analyte detection. Therefore, various mutations have been employed to increase the analyte capture frequency, primarily by altering the electrostatic properties at the entrance. For example, the M2MspA introduced negatively and positively charged residues (D118R/D134R/E139K) within the vestibule and the entrance region of MspA [78]. It reduced the escape of DNA back to the *cis* entrance, thus improving the resolution for DNA base recognition. Besides, the replacement of negatively charged glutamate (E111) with a polar asparagine (N) at the entrance α-HL nanopore obviously increased the DNA translocation frequency [129]. Meanwhile, the α-HL (E111A) prevents ion-pair interaction between E111 and K147, facilitating electrostatic interactions between K147 and sulfonate groups, which in turn enhanced nanoparticle capture [130, 131]. Eliminating the positive charge at the *cis* entrance of α-HL (RL2-A8R/A8K) nanopore reduced DNA translocation frequency by 10-fold compared to the α-HL (WT) nanopore [129]. Upon the RL2-A8R/A8K mutant, alterations of the charged amino acids near the constriction of α-HL, such as the M113R or M113N mutations, significantly increased the DNA translocation. This effect is attributed to the potential electroosmotic flow (EOF) in the bulk solution [129]. Similarly, the ClyA-RR (S110R/D64R) with mutations at both the entrance and lumen facilitates effective DNA translocation [132].

EOF is a pivotal driving force in the regulation of the capture and translocation of non-uniformly charged peptides through nanopores. Enhancement of EOF through specific mutations within the nanopore lumen can significantly increase the capture frequency of these peptides. For example, the AeL (N226Q/S228K) elevates the capture frequency of heterogeneously charged peptides at nearly physiological pH [105]. Moreover, the FraC (D10R/K159E) nanopore recognized oligopeptides, polypeptides, and folded proteins through the promotion of EOF [40]. However, optimizing the balance between high capture rates of individual molecules and reducing translocation speed through the pore constriction is necessary. Since EOF and electrophoretic force (EPF) often act in opposing directions, tailored nanopore modifications are required for specific applications. For instance, the 2E-4D-CytK (K128D/Q145D/S151D/K155D) nanopore has been finely engineered to adjust the distance and ion selectivity along its lumen, resulting in a robust EOF that capable of driving the translocation of polypeptides and proteins against the EPF [43]. Conversely, reducing or eliminating EOF as much as possible is a prevalent strategy for nanopore peptide spectroscopy, particularly for cation-selective nanopore. Under acidic conditions, protonated polypeptides are predominantly captured and transported following the EPF [44].

2.3 Mutations for controlling nanopore structure

Site-directed mutagenesis has been employed to stabilize the open state of nanopore, thereby mitigating interference from baseline noise and gating behavior. For example, the introduction of negative charges into Loop 6 or Loop 1 of the OmpG nanopore, exemplified by the I226D/R228D or V19D/G21E/Y22E/G23D mutants, have modulated the interactions among protonated residues [133, 134]. This manipulation has substantially reduced the random gating caused by pH fluctuations. Moreover, substituting charged residues into neutral Loop 6 effectively stabilized the OmpG nanopore in its open state [134]. Similarly, the cysteine-free ClyA variant (ClyA-SS) exhibits low intrinsic noise in planar lipid bilayer recordings [135, 136]. Additionally, random mutagenesis has been proven to be effective in modulating and stabilizing nanopore structure. For example, the FraC (D10R/K159E) nanopore, generated through random mutagenesis, exhibited WT-level hemolytic activity and effective discrimination of homopolymeric ssDNA [137]. Random mutagenesis has also been utilized to enhance the solubility and stability of ClyA, yielding variants such as ClyA-CS (L99Q/E103G/F166Y/C2885S/K294R) and ClyA-AS (C87A/L99Q/E103G/F166Y/I203V/C285S/K294R/H307Y) [138–141]. These variants were invaluable in monitoring protein conformational changes. The ClyA-AS variant has been widely employed to investigate molecular interactions by trapping individual biomolecules, including proteins and nucleic acids. It offers advantages of a confined reaction environment and ultrahigh sampling frequencies at the single-molecule level. With a well-defined pore size of approximately 10 nm × 7 nm, ClyA-AS is particularly well suited for confinement-based analyses of enzymatic systems. For example, long-observation time electrical recordings of dihydrofolate reductase (DHFR) have revealed that the DHFR has at least four ground-state conformations with distinct ligand affinities [52]. This illuminated how conformational exchange is coupled to catalysis and demonstrated the soft interactions within DHFR [141]. Additionally, this variant enables real-time and single-molecule observation of the co-binding of adenosine triphosphate (ATP)-competitive and allosteric inhibitors

to the Abl kinase [124].

Beyond controlling nanopore stability, altering the subunit-lipid interface could modify the oligomeric composition of nanopore. The W112S and W116S mutations of FraC nanopore weakened the interaction of protein-lipid interface, thereby yielding nanopores with diameters of 1.6, 1.1, and 0.84 nm [22]. These different types of FraC nanopores were allowed to analysis a wide range of peptide lengths. Interestingly, heteromeric pores could also be generated simply by co-incubating two monomeric subunits. A representative example is the YaxAB channel, which exhibits octameric, nonameric, and decameric states. Owing to its deep and long-funneled lumen, the octameric and nonameric YaxAB variants have been applied to single-molecule studies of interactions between proteins and small-molecule [142], as well as protein–protein complexes [143]. These applications highlight the utility of YaxAB nanopores for high-throughput and high-precision drug screening targeting proteins.

2.4 Mutations for hetero-nanopore with single-molecule resolution

Hetero-nanopore represents a powerful platform for advanced single-molecule investigations, significantly expanding the scope of stochastic sensing beyond simple size-exclusion effects to achieve single-site resolution. Typically, hetero-nanopores are generated through co-expression of subunits, followed by electrostatic probe-based gel separation. The heteromeric α-HL (WT_6(N123H, T125H, G133H, L135H)$_1$) nanopore has been employed to simultaneously determine multiple divalent metal ions in solution [144]. The α-HL (M113K)$_3$(M113Y-D8)$_4$ nanopore exhibited distinct differences in residence times and amplitudes for pinacolyl methylphosphonate (PMPA) and cyclohexyl methylphosphonic acid (CMPA), enabling its use in quantifying mixtures of these compounds [145]. Notably, the α-HL (M113R/N139Q)$_6$(M113R/N139Q/L135C)$_1$ nanopore can covalently attach β-cyclodextrin (β-CD) at the L135C and N139Q positions, thereby enabling continuous detection of DNA bases [146]. Furthermore, the α-HL (T117C-D8RL3)$_1$(WT)$_6$ nanopore enables the detection of various nitrogen mustards by leveraging the chemical reactivity of thiol groups at the sole T117C site [120]. Particularly, the single cysteine residue mutated hetero-nanopores were further coupled with various chemical modifications through Michael addition reaction. These engineered nanopores have proven to be highly suitable for monitoring sub-millisecond chemical processes [147], distinguishing chiral isomer [51, 148], and identifying single amino acids in protein sequencing [56]. For instance, the M2MspA (N90C)$_1$(M2)$_7$ coupled with a sole phenylboronic acid or nickel-nitrilotriacetic acid to widely analysis small molecules with diol groups and discriminate amino acids [56, 149, 150]. Recently, Long and co-workers reported an *in situ* strategy to selectively introduce maleimide derivatives into the AeL (K238C) nanopore with a subunit stoichiometric ratio of 3:4 [23]. This method, which utilized steric hindrances to obtain selective modification, might facilitate the customization and expand the diverse chemical functionalities of protein nanopores.

3 Unnatural amino acids modification of protein nanopores

Site-directed mutagenesis primarily involves substituting the 20 canonical amino acids to alter the properties of nanopores. Especially, the cysteine mutagenesis has proven to be effective in introducing chemical modifications. In addition, the incorporation of unnatural amino acids with unique functional groups unlocks vast potential for expanding the capabilities of engineered nanopores. For example, through constructing the K147C variant expression plasmid, the unnatural selenocysteine was incorporated into the lumen of α-HL nanopore using the *E. coli* cysteine auxotrophic system [151]. The selenocysteine in α-HL nanopore was explored as a nanoreactor site to trap the transient intermediates during the catalytic reaction of glutathione peroxidase. Besides, the *in vitro* transcription and translation (IVTT) have been explored to produce α-HL with unnatural amino acids at position 113 [152]. IVTT synthesizes proteins in the test tube, allowing unnatural amino acids to be incorporated by adding aminoacyl-tRNA containing the desired unnatural amino acid (Fig. 3(a)) [153]. Similarly, the genetic code expansion (GCE) technique has been employed to introduce unnatural amino acids into nanopores in *E. coli* cells [24, 154]. This approach involves mutating the codon of the target amino acid to a stop codon and introducing a specific orthogonal aminoacyl-tRNA synthetase-tRNA (aaRS-tRNA) pair (Fig. 3(a)) [155]. The aaRS catalyzes the attachment of an unnatural amino acid to its corresponding tRNA, which then recognizes the stop codon and inserts UAA into the peptide chain. Using GCE, the N^6-carbobenzoxy-L-lysine and N^6-((2-azidoethoxy)carbonyl)-L-lysine have been incorporated into the sensing region of AeL nanopore and the entrance of MspA nanopore, respectively [24, 154]. These modifications enhanced the peptide sensing capability of AeL nanopore and enabled azide-functionalized MspA nanopores to conjugate lysozyme for polysaccharide sensing. Chemical synthesis method also holds tremendous potential for introducing unnatural amino acid side chains (Fig. 3(b)) [156]. Native chemical ligation (NCL) has been reported as a powerful and alternative semi-synthetic strategy to introduce unnatural modifications at arbitrary sites of nanopore [156]. Some studies have successfully employed NCL to incorporate unnatural amino acids with an alkyne group or ketone group into the α-HL nanopore, thereby expanding the range of covalent chemistry that can be examined by the nanoreactor approach (Fig. 3(c)) [156, 157]. However, NCL-based nanopore preparation in general requires complex purification and protein refolding procedures, currently limiting its widespread application.

4 Host–guest chemistry in protein nanopores

Cyclodextrins, particularly β-CD and γ-CD, are generally employed as non-covalently bound adaptor as they can enter the α-HL channel and mediate host–guest interactions with target analytes [158]. The presence of β-CD within the pore modulates the magnitude of ion conductance under applied potential, and then analytes are non-covalently bound to the β-CD via host–guest interactions, leading to characteristic conductance blockages (Fig. 4(a)). The β-CD could lodge at positions of Met113, Lys147, and Glu111 of WT or mutated α-HL pores. Notably, substituting the Met113 residue with asparagine, tryptophan, tyrosine, or phenylalanine has been shown to prolong the residence times of β-CD adaptors within the pore lumen [159, 160]. The α-HL-β-CD complexes have been widely employed for the sensitive detection of various analytes, including PMPA/CMPA mixture [145], ribonucleoside [161], individual nucleotides [13, 146], substrate of trypsin [162], copper ion [163], ATP [164], adenosine monophosphate (AMP) [164], glutathione (GSH) [165], Cd^{2+}-GSH complexes [166], nicotinamide adenine dinucleotide reduced

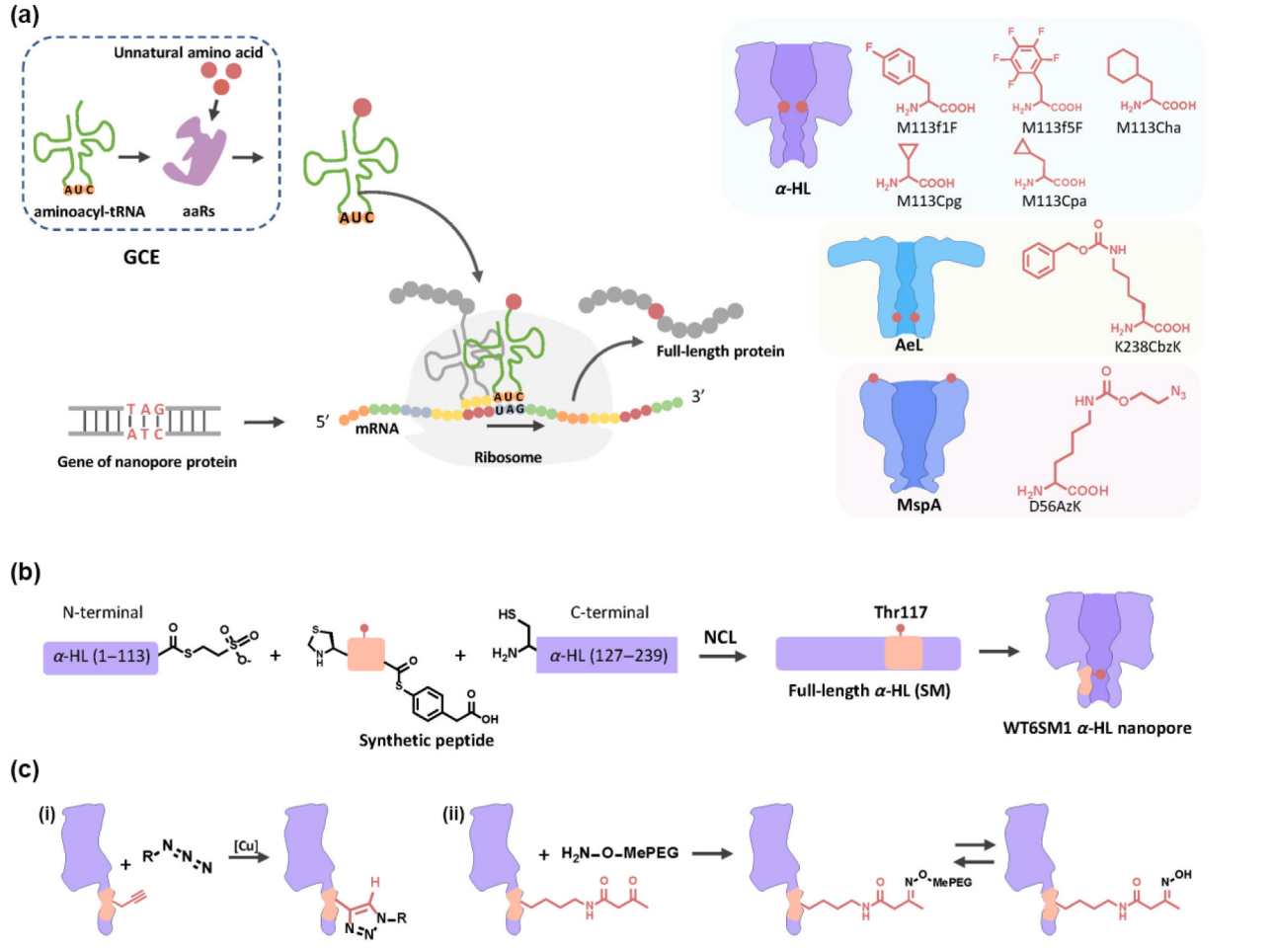

Figure 3 Site-specific introduction of unnatural amino acids into protein nanopores. (a) Genetic engineering methods for incorpoorating unnatural amino acids using aminoacyl-tRNA. The α-HL nanopre was modified via IVTT, while *in vivo* GCE was employed for the AeL and MspA nanopores [24, 152, 154]. (b) NCL was used to incorporate a side chain (orange) containing a specific functional group (red dot) at the Thr117 position in the α-HL nanopre [156, 157]. (c) Unnatural amino acids bearing an (a) alkyne group or (b) ketone group were introduced into the α-HL nanopore, enabling covalent reactions with azide or MePEG-hydroxylamine [156, 157].

form/oxidized form ($NADH/NAD^+$) [167], nerve agent hydrolytes [168], and methylated arginine [169] through host–guest interactions. Moreover, the specific environment provided by β-CD has been leveraged for the chiral discrimination of aromatic amino acids [170] and enantiomers of small molecules (including ibuprofen, thalidomide and duloxetine) [171, 172]. For applications requiring stable adaptor positioning, β-CD adaptors have been covalently attached to the M113C site via a disulfide bond [173]. This modification proves particularly advantageous for continuous nucleotide reading in DNA sequencing, where the covalently attached α-HL-β-CD complex achieves an impressive 99.8% accuracy in identifying nucleoside 5'-monophosphate [146, 173]. Additionally, host–guest interactions have been widely adopted as a common strategy in various nanopore. For example, the stabilized OmpG (G231C/D262C/ΔD215) has equipped with β-CD to quantify adenosine diphosphate (ADP) [174]. The MspA nanopore also exhibits strong interaction with β-CD, with the MspA-β-CD sensor demonstrating effective detection of small organic molecules [175]. In the nanopore-based stochastic sensing utilizing host–guest interactions, γ-CD is also an alternative host molecule. For example, γ-CD has also been lodged in α-HL nanopore to follow the interaction of adamantane carboxylate, as well as identify per- and polyfluoroalkyl substances [176, 177].

Aside from CDs, macrocyclic host molecules with diameters comparable to the α-HL lumen, like cyclic peptides [178], carboxylatopillar[5]arene (CP[5]A) [179], cucurbiturils (CB) [57, 180], and *semiaza*-bambus[6]uril (*semiaza*-BU[6]) [181] have also been explored as adaptors (Fig. 4(a)). These α-HL-host complexes have been investigated as sensors for detecting anions, sequencing peptides, and sensing small molecules. For example, cucurbit[6]uril (CB[6]) could induce reversible current blockages on the *cis* side of the α-HL pore, with the addition of tetrahydrofuran enhancing the blockage current [180]. A truncated cone-shaped sulfonato-calix[4]arene (SC_4), which is smaller than the constriction of α-HL nanopore, has also been utilized to functionalize the pore for real-time sensing of the interaction between SC_4 and 4, 4'-dipyridinium-azobenzene [182]. The $(N\text{-hydroxypropyl})_6$-*semiaza*-BU[6] acted as anino receptors for quantify chloride ions. The cucurbit[7]uril (CB[7]) adaptor could be modified with a DNA probe or peptide, hence sensing the DNA probe or amino acids in the peptide (Fig. 4(b)) [57, 183]. Interestingly, the integration of cage-like host molecules such as CB with nanopore single-molecule measurements enables the establishing of a nanocage-based exchange system, allowing direct and precise measurement of weak interactions. For example, CB[7]-modified α-HL nanopores have been used to examine the CH–π interactions between phenylalanine derivatives and aliphatic amino acids [184], as well as the π–π interactions between phenylalanine derivatives [185],

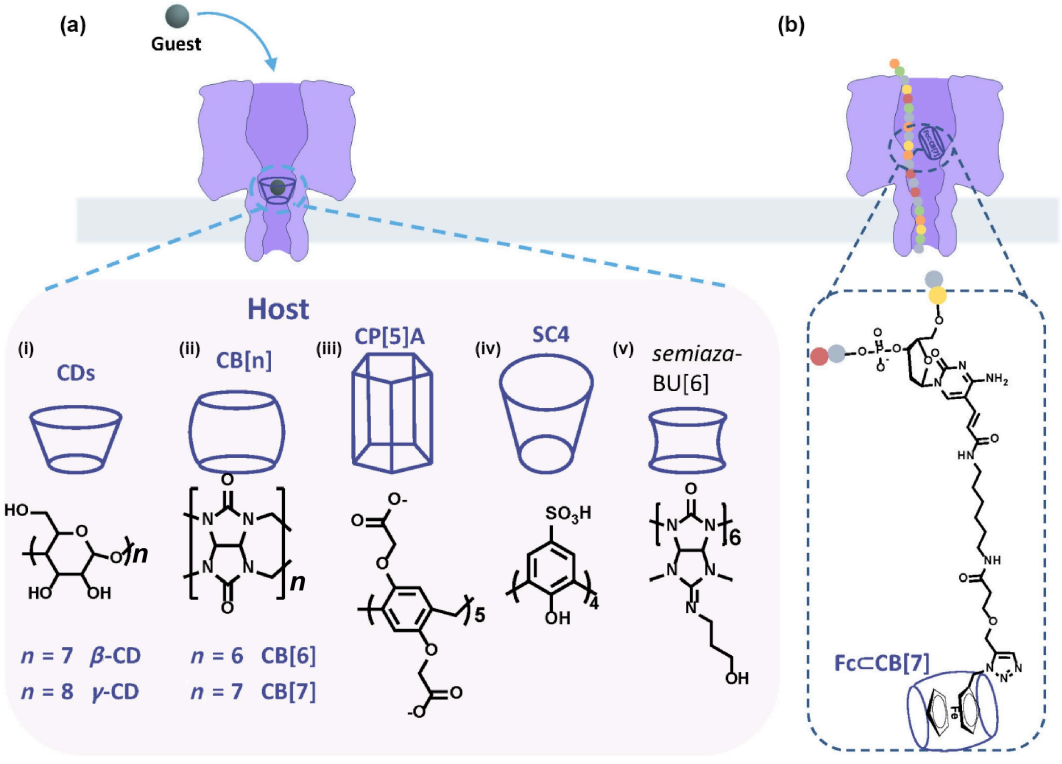

Figure 4 Strategies for sensing analytes through host–guest interactions. (a) Enhancement of host–guest interactions by equipping with ring-shaped host molecules into the α-HL nanopore. The structures and shapes of (a) β-CD and γ-CD; (b) CB[6] and CB[7]; (c) CP[5]A; (d) SC4; (e) *semiaza*-BU[6] [57, 158, 176, 179–182]. (b) Covalent attachment of a ferrocene⊂cucurbit[7]uril (Fc⊂CB[7]) host to a DNA strand, generating characteristic current events as the modified DNA passing through the α-HL nanopore [183].

revealing that both interactions are primarily governed by dispersive forces.

5 Chemical modification of protein nanopores

Chemical modification has attracted increasing attention in the detection of small molecules, as it enables identification of enantiomers or detection of reactive behavior of organic molecules. Michael addition and click chemistry reactions are two widely used strategies for introducing chemical modifications. Bioconjugate chemistry can also be applied to incorporate reactive handles and photo-active groups. Overall, chemical functionalization of nanopores is typically achieved through site-directed mutagenesis, where a cysteine mutation is always a prerequisite for chemical modifications (details are in Section 2.1).

Introducing reactive group within the pore is an efficient approach for sensing small molecules. For example, copper(II)-phenanthroline group was linked at the position 117 via a disulfide bond reaction within α-HL (T117C) nanopore (Fig. 5(a)) [148, 186]. This chemically modified α-HL nanopore enabled real-time detection of a broad range of neurotransmitters and the chiral discrimination of amino acid. Similarly, a boronic acid group was introduced at position 117, allowing the engineered α-HL nanopore to distinguish isomers of D-glucose and D-fructose through the reversible formation of boronate esters [187]. Phenylboronic acid (PBA) has demonstrated powerful and versatile performance in nanopore-based detection of small molecules through reversibly covalent interactions. For instance, the MspA-PBA nanopore, engineered through the Michael addition reaction between maleimide and cysteine of N90C site, has been extensively applied to discriminate various monosaccharide [149], disaccharides [150], alditols [188], glucose [189], nucleotide sugars [190], ribonucleoside [191], nucleoside monophosphates and their epigenetic modifications [12], as the vicinal diols of these analytes chemically reacted with the boronic acid group (Fig. 5(b)). Similarly, the spontaneous interconversion between chiral configurations of boronic esters within the MspA-PBA nanopore was observed upon addition of *cis*-diol compound [51]. This property was utilized to identify *cis*-diols in alcoholic samples, allowing the generation of unique signatures for different beverages [192]. Furthermore, N-acetyl modification on ribonucleotides, histones, and glucosamine could be detected, as N-acetylation produces acetohydroxamic acid, which then reacts with the boronic acid group of MspA-PBA [193]. Aside from PBA, nitrilotriacetic acid (NTA) could also be used to modify the MspA nanopore at the N90C site via the Michael addition reaction (Fig. 5(b)) [19, 56, 194]. With the chelation of Ni^{2+} ion, the MspA-NTA nanopore has been used to identify vitamins, representative thyroid hormones, all 20 amino acids, and four modified amino acids. Notably, the identification of amino acids by the MspA-NTA nanopore reached 98.6% accuracy when combined with machine learning algorithm, making a significant advancement in protein sequencing by nanopore. Moreover, the MspA-NTA nanopore could discriminate rare earth element (REE) ions through chelation with these REE ions and another NTA ligand [195]. Interestingly, chemical modification at the non-constriction site in lumen, such as the periplasmic side of the OmpF nanopore (E181C), could not only quantify the transport of norfloxacin at biological relevant concentrations, but also identify permeation across the nanopore [196].

Beyond enabling diverse detection principles and broadening the

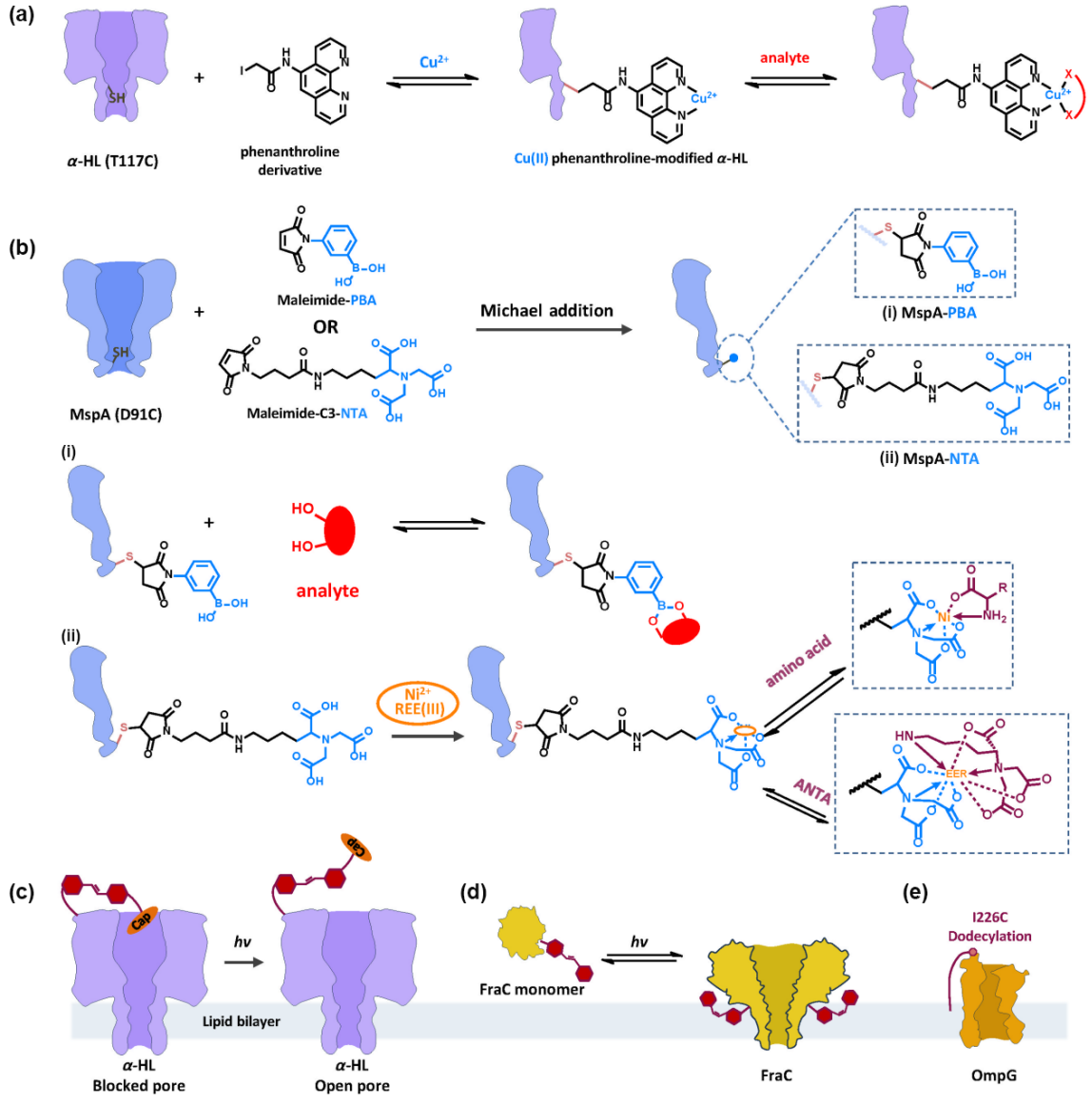

Figure 5 Chemical modifications in protein nanopores to enhance functionality. (a) Copper(II)-phenanthroline group linked to the α-HL (T117C) nanopore, enabling reversible binding of analytes (red) to the copper(II) within the functionalized nanopore [148, 186]. (b) Thiol group in MspA (D91C) reacted with maleimide-phenylboronic acid (Maleimide-PBA) or maleimide-C3-nitrilotriacetic (Maleimide-C3-NTA) via Michael addition to form thioether adducts [12, 19, 56, 149]. The functionalized MspA-PBA nanopore (a) formed reversible boronate esters with anlytes containing vicinal diols (red), while the MspA-NTA nanopore (b) chelated with Ni^{2+} ion or REE ions (orange ring) for the detection of amino acids or REEs [56, 149, 150, 195]. (c) α-HL nanopore functionalized with a photoswitch (red) in *trans*-azobenzene (blocked state) and *cis*-azobenzene (open stste) configurations [198]. (d) Assembly of a photocontrolled FraC nanopore: The FraC nanopoore with a photoswitch (red) did not bind to the lipid bilayer in the *trans*-azobenzene state, and formed a pore upon switching to the *cis*-azobenzene state via light irradiation [200]. (e) Pinning of OmpG nanopore loop to the lipid bilayer through dodecylation at the I226C residue (red) of loop 6 [201].

range of detectable analytes through incorporation of reactive groups within the pore cavity, chemical modification of nanopore with environmentally sensitive groups can further regulate the assembly and conductivity properties of nanopore. For example, a photo-caged 7-(diethylamino)-4-(hydroxymethyl)-coumarin moiety could be incorporated into the lumen of OmpG (ΔL6/M13C/E154C) [197]. The presence of the photo-caged molecule reduced the conductivity of the OmpG nanopore, and light-induced cleavage effectively regulated its conductivity properties. Similarly, a photo-switchable azobenzene group was covalently attached to the cap domain of α-HL nanopore [198]. In this case, the photo-active compound with a long arm obstructed the vestibule, and the light-induced isomerization of the azobenzene moiety modulated the transport properties of α-HL nanopore (Fig. 5(c)). Except switching ion permeation, the introduction of photo-active compounds into nanopore enables the regulation of nanopore assembly by light. Bayley and colleagues attached a photo-caged α-carboxy-2-nitrobenzyl group to the glycine-rich central loop of the α-HL (R104C) nanopore [199]. Since the binding of α-carboxy-2-nitrobenzyl group to the loop interferes with the transmembrane fusion capability, photolysis dissociates the modified group and allows the uncaged α-HL to penetrate the membrane and form functional pores. In a similar manner, an azobenzene group was covalently linked to the Y138C residue on the α2 helix of FraC nanopore (Fig. 5(d)) [200]. As a result, this engineered nanopore achieved reversible light-controlled assembly

due to the photo-controlled azobenzene moiety, exhibited potential applications in photopharmacology, particularly in cancer therapeutics.

Chemical modification of nanopores also plays a significant role in mitigating gating behavior. For example, pinning Loop 6 to the membrane through dodecylation at position 226C of OmpG provides an effective strategy, resulting in a constitutively open OmpG nanopore (Fig. 5(e)) [201].

In general, the most common strategy for introducing site-specific chemical modifications into the surfaces or lumen of protein nanopores remains cysteine-based bioconjugation. The typical workflow involves selecting a targeting site, presenting a cysteine mutation, obtaining the mutant, and performing the bioconjugation. For heteropolymeric channels, an additional purification step is usually required. A variety of bio-orthogonal ligation methods have been developed, including reactions involving cysteine thiols with maleimides [202], lysine ε-amines with N-hydroxysuccinimide (NHS) esters and their sulfonated analogues [202, 203], N-terminal amino groups with 2-ethynylbenzaldehydes (2-EBA) [204], electron-rich tyrosine residues with benzenediazonium species [205], and methionine S-Me groups with tailored hypervalent iodine reagents [206], many of which already achieve high sensitivity and selectivity. From the perspective of reactivity and practical reaction conditions, nucleophilic conjugation involving cysteine and lysine remains the most widely used approach. However, the high natural abundance and broad surface accessibility of lysine residues make precise site control difficult to achieve [202]. Consequently, cysteine-based coupling reactions remain the predominant strategy for site-specific chemical modification of proteins, and this trend is also reflected in the chemical functionalization of protein nanopores.

We systematically compared three commonly used modification strategies based on gene and protein engineering (Table 1). Although site-directed mutagenesis remains the most accessible and widely applied approach, enabling efficient and versatile functionality of nanopores for diverse applications, more complex modification strategies are often required when targeting a broader range of small molecules. While the applicability of these advanced strategies continues to expand, they are generally less efficient and less cost-effective than site-directed mutagenesis. Nevertheless, cysteine-based chemical modifications, including click reactions and other orthogonal conjugation methods, are receiving increasing attention. We anticipate that it will play an increasingly important role in future nanopore engineering.

6 Truncation of protein nanopores

Nanopores exhibit atomically precise nano- or sub-nanometer dimensions determined by their protein sequences. Consequently, truncation of amino acids typically affects the delicate assembly and stability of the nanopore, resulting in significant changes in pore size, membrane fusion stability, and intrinsic noise. The truncation of flexible loops also offers an optional and effective strategy for producing stable biological nanopores. For example, the constructed FhuA ΔC/Δ4L nanopore, which removes the N-terminal 160-residue cork domain (C) and loops 3, 4, 5 and 11, maintains gating-free, open state across a broad range of conditions [207–209]. As a result, this rationally designed FhuA nanopore has been developed as a single-molecule probe for tracking pepsin digestion and studying protein-DNA aptamer interactions [207]. Additionally, stepwise duplication of two β-strands from the FhuA ΔC nanopore could further expand the pore diameter [210]. Moreover, another variant, TL-FhuA nanopore (ΔC/ΔL3, L4, L5, L10, L11) with the N-terminal hexahistidine arm was engineered to achieve higher single-channel conductance and demonstrate sensitivity in capturing monoclonal antibody with anti-His tag [211]. Through electrostatic stabilization via truncation, deletion of several residues near the flexible loop 6 of OmpG (Δ221-227/R228G/ΔD215) led to the development of a quiet ΔL6-ΔD215 OmpG nanopore with an improved open-state lifetime [212]. Additionally, the Y209C mutation in this ΔL6-ΔD215 OmpG nanopore enabled the detecting and distinguishing of small molecules, such as ATP and L-glutamate [212]. Similarly, truncation of the N-terminus 15 amino acids of CymA nanopore rendered it electrically silent, enabling efficient identification of the

Table 1 Comparison of the commonly used modification strategies (site-directed mutagenesis, unnatural amino acids modification and chemical modification)

Strategies	Ways	Challenges	Typical functional groups	Throughput	Optimal application
Site-directed mutagenesis	Homopolymeric protein	·Easy operation	·Charged/uncharged amino acids (D, N, E, Q, R, K) ·Aromatic amino acids (F, W, Y) ·Metal coordination amino acids (M, H) ·Covalent modification (C)	·Standard workflow ·Parallelization	·DNA/RNA sequencing ·Peptides sensing ·Amino acids identification ·Nanoreactor
	Heteropolymeric protein	·Controlled assembly ·Purification		·Complex workflow	
Unnatural amino acids	cysteine auxotrophic system	·Cysteine-auxotrophic strain ·Controlled assembly	·Selenocysteine	·Complex workflow	·Trapping the intermediates of catalytic reaction as a nanoreactor
	IVTT/GCE	·Low throughput ·Low efficiency ·Missense mutation ·Higher costs	·N6-carbobenzoxy-L-lysine (Carbobenzoxy) ·N6-((2-azidoethoxy)carbonyl)-L-lysine	·Complex workflow ·Output < μg/mL	·Enhancing the resolution for peptides ·Polysaccharide sensing
	NCL	·Protein refolding ·Purification	·Alkyne group or ketone group	·Complex synthetic chemistry	·Constructing nanoreactor
Chemical modification	Cysteine-based coupling reaction	·Easy operation ·Competitive response	·Phenanthroline group ·Boronic acid group ·Nitrilotriacetic acid ·Photo-caged 7-(diethylamino)-4-(hydroxymethyl)-coumarin ·Azobenzene group ·α-carboxy-2-nitrobenzyl group ·Dodecyl	·Standard workflow ·Parallelization	·Identification of enantiomers and rare earth element ions ·Photopharmacology, and cancer therapeutics

EOF of neutral α-cyclodextrin molecules through nanopore sensing [213, 214]. Beyond N-terminal deletions, truncating two to ten amino acids in the transmembrane β-barrel of the α-HL produced functional pores in lipid bilayers [215], preserving the internal structures of the WT α-HL nanopore and potentially enhancing base discrimination. Further mutation (M113G) of this α-HL truncation enabled tight binding of β-CD and facilitated the recognition of individual nucleobase through host–guest interaction [216]. Besides, deletion of amino acids at the C-terminus (Δ287–309) or in the internal channel loop (Δ229–246) of the phi29 channel expanded its capability to detect peptides with propionylation modifications [217].

7 Outside probes modification of protein nanopores

Constructing tethered baits at the entrance of nanopores is an efficient strategy to selectively capture analytes. It converts the biological information of the capture and release process into distinct electrical signatures. Commonly, DNA, peptides, coenzymes, antigens, and antibodies are employed to engineer nanopore-tether systems via chemical or genetic modifications. Early advancements in tethered bait engineering included attaching a polyethylene glycol (PEG) chain with a biotin molecule into the lumen of heteroheptameric α-HL $(S106C)_1(WT)_6$ nanopore through disulfide exchange reaction [48]. This biotin-functionalized nanopore captured streptavidin (SA), SA-modified analytes and anti-biotin antibodies, enabling their identification and quantification through distinct current signatures. Similarly, a high-affinity biotin was linked to Cys224 on loop 6 of OmpG through a reaction between cysteine residues and maleimide [218]. This biotinylated OmpG nanopore could discriminate anti-biotin antibody homologues and glycosylated avidin isoforms (Fig. 6(a)) [219–221]. Additionally, the length of the PEG tether linking the biotin to the OmpG nanopore was found to influence the sensitivity and selectivity for protein detection [222].

With the rapid advancement of bioorthogonal reactions, such as click chemistry, it has become increasingly straightforward and widely adopted to modify DNA or peptides on the surface of nanopore, further expanding the applications of nanopore stochastic sensing. For instance, ssDNA oligonucleotides were covalently attached to the single cysteine residue of the heteroheptameric α-HL $(17C\text{-}D4)_1(WT)_6$ nanopore, facilitating the detection of complementary DNA strands, the study of DNA duplex formation kinetics, and sensing the depth of the α-HL lumen (Fig. 6(b)) [223–225]. Furthermore, these DNA strands were further designed as aptamers to target and quantify proteins, like thrombin, with high selectivity [226]. Similarly, the OmpG (D224C) nanopore has been chemically tethered to a short ssDNA or peptide at Cys224 for sensing complementary DNA or proteins [134, 227]. Additionally, DNA aptamers were conjugated to the ClyA (S110C) near the pore entrance, enabling the selective capture and differentiation of human and bovine thrombin, which share 86% sequence identity [136]. Furthermore, several nanobodies have been attached to the S110C residue of ClyA nanopore through DNA linkers (Fig. 6(c)) [47]. This functionalized ClyA nanopore demonstrated the capability to specifically recognize protein biomarkers of varying sizes, including the large SARS-CoV-2 spike

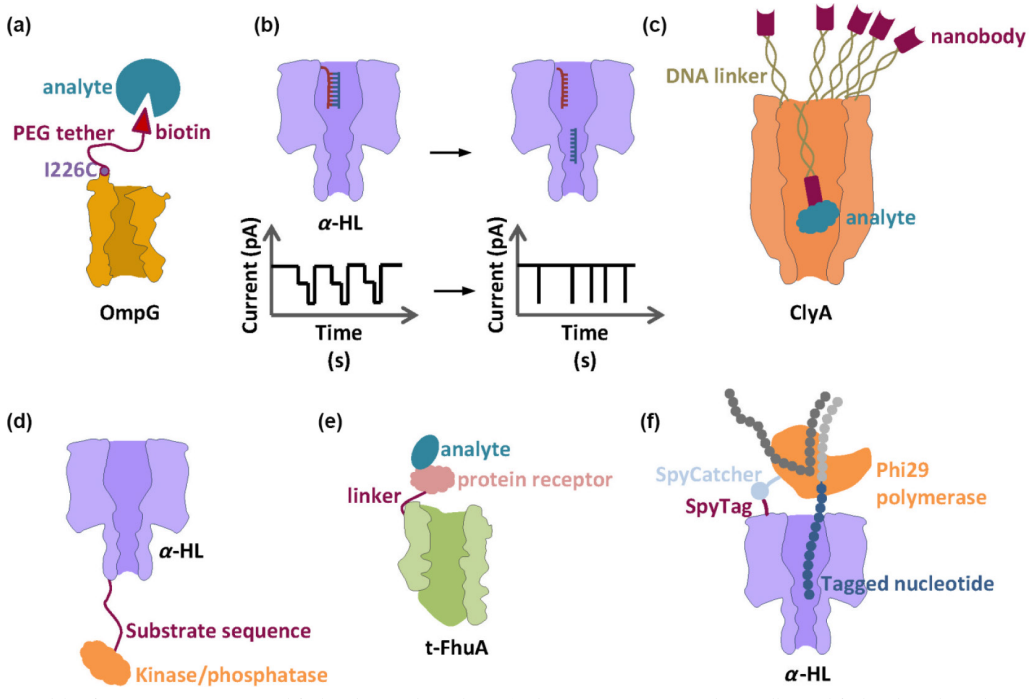

Figure 6 Schemstic models of protein nanopores modified with outside probes. (a) The OmpG nanopore chemically modified with maleimide-PEG-biotin (red) at the I226C position [219, 220]. (b) The α-HL nanopore chemically modified with a hexamethylene-tagged DNA oligonucleotide (red) via a disulfide bond, which responded to individual binding events with oligonucleotides of complementary sequence (blue) [224]. (c) The ClyA nanopore chemically modified with DNA oligonucleotides (brown) through maleimide-PEG4-DBCO linkers, with the nanobodies (red) immobilized on the ClyA nanopore by DNA strand hybridization [47]. The functionalized probes changed conformation in response to analyte (blue) binding. (d) The genetically engineered α-HL nanopore fused with a single substrate peptide (red), enabling binding to protein kinases or phosphatases (orange) [231, 232]. (e) The t-FhuA nanopore chemically modified with a protein receptor (pink) through a flexible $(GGS)_2$ tether (red) [235, 236]. (f) The genetically engineered α-HL nanopore fused with a SpyTag (red), which covalently attached phi29-SpyCatcher (light grey and orange) to construct a nanopore-polymerase sequencing engine [240, 241]. This engine sequenced single-molecule DNA using tagged nucleotides.

protein, the medium-sized human epidermal growth factor receptor 2 (HER2) receptor, and small murine urokinase-type plasminogen activator (muPA).

In addition to link the outside probes through chemical reactions, the peptides tethered nanopore could also be prepared by genetic engineering. For instance, peptides fused at the C-terminus of phi29 channel, such as the urokinase-type plasminogen activator receptor (uPAR) binding peptide, galectin3 (GAL3), epithelial cell adhesion molecule (EpCAM) peptide, and Thomsen-Friedenreich (TF) binding peptide, enabled it to be an outside probe for directly detecting cancer biomarkers via antibody or adaptor binding [228–230]. Additionally, the protein kinase peptide inhibitor (PKIP) sequence was genetically encoded to the *trans* entrance (between T125 and G134) of α-HL, preparing the heteroheptameric α-HL $(PKIP)_1WT_6$ nanopore, which effectively detected the catalytic subunit of protein kinase A (Fig. 6(d)) [231]. Similarly, genetically encoding proviral integration site for moloney murine leukemia virus (PIM) kinase or protein phosphatase substrates into α-HL generated heteroheptameric $(D127N\text{-peptide-TEV})_1(D127N)_6$ nanopores for further screening kinase inhibitors and detecting peptide phosphorylation or dephosphorylation [232–234]. Bulky protein could also be an outside protein modified at the entrance of nanopore to capture and sense analytes. For example, a truncated FhuA nanopore fused with a N-terminus barnase (Bn) protein receptor via a $(GGS)_2$ hexapeptide linker (OBn$(GGS)_2$t-FhuA) specifically captured the peptide inhibitor and detected the kinetics of barnase-barstar interactions (Fig. 6(e)) [235–237]. Similarly, a modified t-FhuA nanopore, fused with a cellular rapidly accelerated fibrosarcoma-RAS binding domain and antibodies, enabled selective and sensitive proteins detection [238, 239].

Notably, native proteins could also be tethered to nanopore surfaces to construct stochastic sensor. For instance, phi29 polymerase was conjugated to the *cis* entrance of α-HL nanopore embedded in a lipid bilayer of chips via SpyCatcher/SpyTag system (Fig. 6(f)) [240, 241]. This assembly configuration enabled real-time detection of tagged nucleotides on DNA template [240]. Significantly, this platform has been applied to detect over 200 tagged-nucleotide signals with error rate below 1.2% [241]. Moreover, the platform also facilitated polymerase variants screening using barcoded DNA template [242].

8 Redesign of protein nanopore

Computational and customized designs hold great potential for generating nanopores with tailored functions, as demonstrated by several innovative cases. For example, replacing the $\beta1$–$\beta6$ strands of OmpF nanopore with the corresponding strands from OmpG enriched the lipid-facing motifs, resulting in the OmpGF chimera nanopore [243]. This design enhanced the stability of the transmembrane region of OmpF, allowing the protein to refold into a β-sheet nanopore with increased conductance. In addition, a fusion of the mobile loop of co-chaperonin GroES between Glu228 and Lys289 of the α-HL nanopore not only retained the pore-forming ability but also enabled binding to the chaperonin GroEL (Fig. 7(a)) [244]. This α-HL-GroES modular nanopore facilitated the study of kinetic intermediates in the GroEL-GroES chaperonin system. Similarly, a notable example is the construction of a dual-constriction CsgG-CsgF nanopore, in which the 33 N-terminal residues of CsgF bind inside the β-barrel of the CsgG pore (Fig. 7(b)) [245]. This CsgG-CsgF nanopore improved signal and base-calling accuracy in the homopolymer regions, and it owns a dual-constriction to modulate electrical signal during ssDNA translocation, resulting in a 25%–70% improvement in single-read accuracy for homopolymers up to 9 nucleotides long. Notably, the improved resolution conferred by the dual-constriction of CsgG-CsgF also holds the potential for protein sequencing via a "thread-and-read" approach [80, 82, 89, 246]. Recently, the size-tunable nanopores have been constructed through assembling the α-helcal peptide (IWza) on cyclodextrins with different numbers of subunits (Fig. 7(c)) [247]. These $(IWza)_n$-CD pore could sense saccharide

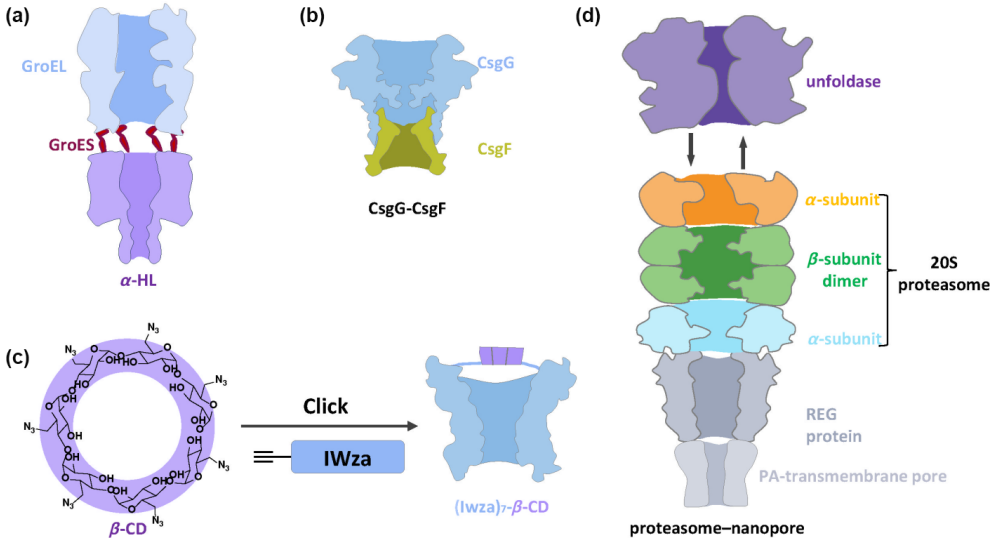

Figure 7 Redesign of co-chaperonin nanopores. (a) A nanopore-GroES was engineered by genetically fusing the α-HL nanopore with the flexible loops of GroES (red) [244]. The fused GroES loops retained the ability to bind a single-ring variant of the GroEL protein-folding chaperonin (blue). (b) The dual-constriction CsgG-CsgF nanopore was engineered by genetically fusing the CsgG nanopore (blue) with its extracellular interaction partner, CsgF (olive green) [245]. (c) The size-tunable nanopore was constructed through chemically linking cyclodextrins and IWza peptide [247]. (d) Schematic representation of a proteasome-nanopore fabricated from three distinct domains: The anthrax-derived β-barrel (light grey) was genetically fused to the proteasome activator 28α (also called REG) protein (grey) and the α-subunit of 20S proteasome (blue) [62]. The β-subunit (green) and another α-subunit of the 20S proteasome were noon-covalently assembled to form 20S proteasome. The proteasome-nanopore further bound an unfoldase (purple) to catalyze the unfolding and translocation of proteins.

chitosan with molecular weight ranging from 60,000 to 12,000, as well as the guest molecule (1-amantadine hydrochloride). This study provided a method for directed assembly of protein nanopores though template molecule and artificial peptide. Maglia's group demonstrated a groundbreaking example of a proteasome-nanopore fabricated from three distinct domains: the truncated transmembrane region of bacterial protective antigen, the proteasome activator 28α, and the archaeal 20S proteasome. The truncated valosin-containing protein-like ATPase of *T. acidophilum* (VATΔN) was selected as the motor protein to recognize and unravel substrates (Fig. 7(d)) [62]. This molecular machine supports two potential modes of single-molecule protein analysis: the "chop-and-drop" approach, which identifies unfolded proteins via peptide mass fingerprinting, and the "thread-and-read" mode, where peptides are ratcheted through the nanopore. This bottom-up fabrication approach, which integrates multiple proteins into molecular machines with diverse functions, lays the groundwork for the expansion of nanopore applications, particularly in the development of advanced native protein sequencing techniques, such as de novo chain sequencing. However, this modular system has successfully detected the translocation of unfolded peptides, but it has not yet achieved single-amino-acid resolution.

9 Conclusions and outlook

In the past two decades, significant advancements have been made in the development of protein nanopores for applications in DNA sequencing, protein sequencing, and single-molecule detection. Modifications to these nanopores have greatly enhanced their sensitivity, stability and specificity. Despite these advances, the range of detectable analytes remains constrained, necessitating both refinement of existing nanopores and discovery of novel channels to broaden applications. The introduction of small molecules and unnatural amino acids at the sensing residues has greatly expanded the chemical diversity and functionality of nanopores. For instance, the incorporation of nickel-nitrilotriacetic acid into MspA nanopores has enabled the detection of all 20 natural amino acids, providing insights into exopeptidases-based protein sequencing [56]. While the introduction of unnatural amino acids remains rare due to challenges in their incorporation into nanopores via genetic or semisynthetic methods. Future developments in synthetic molecular biology may enable more extensive use of unnatural amino acids, leveraging their diverse chemical properties. Furthermore, computational nanopore redesign has shown great promise in creating template-base precise modular nanopores with specific functions. A notable example is the bottom-up constructing of protease-nanopore, which facilitates both protein unfolding and fragment peptide detection [63]. Recently, several novel nanopores have been identified, such as the truncated E1 helicase from bovine papillomavirus, which could simultaneously unwind and translocate DNA strands [248], and a mechanosensitive small-conductance channel from *Pseudomonas aeruginosa*, which has shown the capability for continue detection of antibiotics *in vivo* [30, 249]. Beyond discovering natural membrane proteins, de novo design of synthetic nanopores offers unparalleled control over channel properties, increasingly realized through artificial intelligence-driven advances in protein engineering, exemplified by the successful creation of functional α-helical barrels [38, 39, 250] and the de novo SVG28 β-barrel nanopore that detects oligopeptides [251].

Achieving single-molecule protein sequencing remains one of the biggest challenges in nanopore stochastic sensing. Although artificial intelligence-based de novo methods appear to offer a promising approach for fabricating protease-nanopore systems, there still remains significant challenges. These include the complex assembly of motor proteins and nanopores, the enhancement of the spatial and temporal resolution of nanopores, and the lack of effective solutions for decoding electrical signals amidst background noise and mutual interference. Specifically, the intrinsic complexity of peptides makes signal interpretation far more difficult than in DNA sequencing. The ionic current reflects the combined influence of decade amino acids (~ 17 in CsgG) [252] within the nanopore constriction, producing an enormous number of possible signal patterns. This combinatorial complexity obscures the contributions of individual amino acids, lowers the SNR, and results in a highly convoluted relationship between signal and sequence [60]. Moreover, polypeptide chains derived from full-length proteins tend to coil and fluctuate within the nanopore lumen because they experience nonuniform stretching forces. As a result, identical sequences do not always produce reproducible or clearly distinguishable signals. Currently, there still lack large-scale, high-quality training datasets, which significantly limits the development of supervised learning models for robust protein sequence decoding.

Overcoming these bottlenecks will require coordinated progress in both nanopore sensing system design and computational algorithms. High-performance sensing architectures are prerequisites for achieving single-amino acid resolution and accurate signal decoding. Examples include nanopores engineered with ultrathin constrictions or multiple reading heads analogous to DNA sequencing [62, 253] that enable residue-by-residue identification, and systems inspired by earlier successes in discriminating 20 amino acids through metal chelation [55, 56] or host–guest interactions [57], which suggest that strengthening specific interactions between engineered nanopore components and individual residues may be a promising route. In addition, denaturing environments such as guanidinium salts or urea can help maintain a more linear conformation of peptides in the electrolyte [254–256], thereby improving signal uniformity. At the algorithmic level, very few studies have addressed protein nanopore signal decoding. Drawing on advances in third-generation DNA sequencing, researchers now deploy neural-network architectures, convolutional, long short-term memory, and transformer models, through tools such as Chiron [257], CATCaller [258], DEMINERS [259], and ONT pipelines like Guppy and Dorado, which may allow protein nanopore sequencing to bypass the earliest developmental challenges and move more rapidly toward a phase of accelerated progress. Collectively, the authors believe that these challenges in nanopore protein sequencing will eventually be overcome with further advancements in protein nanopore structural modifications, along with innovative applications and the rapid evolution of interdisciplinary fields, particularly artificial intelligence driven structural design and electrical signal decoding technologies.

Data availability

Not applicable.

Acknowledgements

This work is granted by the National Natural Science Foundation of China (Nos. 32301258, and 32372420), Natural Science Foundation of Sichuan, China (No. 2024NSFSC1185), China Postdoctoral Science Foundation (Nos. 2023TQ0230, GZB20230484, and 2024M752201), Post-Doctor Research Project, West China Hospital, Sichuan University (No. 2024HXBH123).

Declaration of competing interest

All the contributing authors report no conflict of interests in this work.

Author contribution statement

K. S.: Conceiving the outline, writing manuscript, funding acquisition. M. Z. W.: Writing manuscript. Y. X.: Revising manuscript. Y. L.: Writing manuscript. M. H. L.: Revising manuscript. J. N. W.: Revising manuscript. Y. J.: Writing manuscript. S. L. Z.: Conceiving the outline. J. G.: Project administration.

Informed consent

Not applicable.

Ethics statement

Not applicable.

Use of AI statement

None.

References

[1] Deamer, D.; Akeson, M.; Branton, D. Three decades of nanopore sequencing. *Nat. Biotechnol.* **2016**, *34*, 518–524.

[2] Bayley, H. Nanopore sequencing: From imagination to reality. *Clin. Chem.* **2015**, *61*, 25–31.

[3] Quick, J.; Loman, N. J.; Duraffour, S.; Simpson, J. T.; Severi, E.; Cowley, L.; Bore, J. A.; Koundouno, R.; Dudas, G.; Mikhail, A. et al. Real-time, portable genome sequencing for Ebola surveillance. *Nature* **2016**, *530*, 228–232.

[4] Wang, Y. H.; Zhao, Y.; Bollas, A.; Wang, Y. R.; Au, K. F. Nanopore sequencing technology, bioinformatics and applications. *Nat. Biotechnol.* **2021**, *39*, 1348–1365.

[5] Lu, H. Y.; Giordano, F.; Ning, Z. M. Oxford nanopore MinION sequencing and genome assembly. *Genomics, Proteomics Bioinformatics* **2016**, *14*, 265–279.

[6] Marx, V. Method of the year: Long-read sequencing. *Nat. Methods* **2023**, *20*, 6–11.

[7] Shi, W. Q.; Friedman, A. K.; Baker, L. A. Nanopore sensing. *Anal. Chem.* **2017**, *89*, 157–188.

[8] Majd, S.; Yusko, E. C.; Billeh, Y. N.; Macrae, M. X.; Yang, J.; Mayer, M. Applications of biological pores in nanomedicine, sensing, and nanoelectronics. *Curr. Opin. Biotechnol.* **2010**, *21*, 439–476.

[9] Wu, Y. F.; Gooding, J. J. The application of single molecule nanopore sensing for quantitative analysis. *Chem. Soc. Rev.* **2022**, *51*, 3862–3885.

[10] Venkatesan, B. M.; Bashir, R. Nanopore sensors for nucleic acid analysis. *Nat. Nanotechnol.* **2011**, *6*, 615–624.

[11] Wang, J. J.; Li, M. Y.; Yang, J.; Wang, Y. Q.; Wu, X. Y.; Huang, J.; Ying, Y. L.; Long, Y. T. Direct quantification of damaged nucleotides in oligonucleotides using an aerolysin single molecule interface. *ACS Cent. Sci.* **2020**, *6*, 76–82.

[12] Wang, Y. Q.; Zhang, S. Y.; Jia, W. D.; Fan, P. P.; Wang, L. Y.; Li, X. Y.; Chen, J. L.; Cao, Z. Y.; Du, X. Y.; Liu, Y. et al. Identification of nucleoside monophosphates and their epigenetic modifications using an engineered nanopore. *Nat. Nanotechnol.* **2022**, *17*, 976–983.

[13] Ayub, M.; Hardwick, S. W.; Luisi, B. F.; Bayley, H. Nanopore-based identification of individual nucleotides for direct RNA sequencing. *Nano Lett.* **2013**, *13*, 6144–6150.

[14] Niu, H. Y.; Li, M. Y.; Gao, Y.; Li, J. G.; Jiang, J.; Ying, Y. L.; Long, Y. T. Direct mapping of tyrosine sulfation states in native peptides by nanopore. *Nat. Chem. Biol.* **2025**, *21*, 716–726.

[15] Lucas, F. L. R.; Sarthak, K.; Lenting, E. M.; Coltan, D.; van der Heide, N. J.; Versloot, R. C. A.; Aksimentiev, A.; Maglia, G. The manipulation of the internal hydrophobicity of FraC nanopores augments peptide capture and recognition. *ACS Nano* **2021**, *15*, 9600–9613.

[16] Wloka, C.; Van Meervelt, V.; Van Gelder, D.; Danda, N.; Jager, N.; Williams, C. P.; Maglia, G. Label-free and real-time detection of protein ubiquitination with a biological nanopore. *ACS Nano* **2017**, *11*, 4387–4394.

[17] Chanakul, W.; Mukhopadhyay, A.; Awasthi, S.; Protopopova, A. D.; Ianiro, A.; Mayer, M. Large and stable nanopores formed by complement component 9 for characterizing single folded proteins. *ACS Nano* **2025**, *19*, 5240–5252.

[18] Ouldali, H.; Sarthak, K.; Ensslen, T.; Piguet, F.; Manivet, P.; Pelta, J.; Behrends, J. C.; Aksimentiev, A.; Oukhaled, A. Electrical recognition of the twenty proteinogenic amino acids using an aerolysin nanopore. *Nat. Biotechnol.* **2020**, *38*, 176–181.

[19] Wang, K. F.; Yang, X.; Xiao, Y. Q.; Cao, Z. Y.; Zhang, S. Y.; Zhang, P. K.; Huang, S. Simultaneous identification of major thyroid hormones by a nickel immobilized biological nanopore. *Nano Lett.* **2024**, *24*, 305–311.

[20] Galenkamp, N. S.; Soskine, M.; Hermans, J.; Wloka, C.; Maglia, G. Direct electrical quantification of glucose and asparagine from bodily fluids using nanopores. *Nat. Commun.* **2018**, *9*, 4085.

[21] Lucas, F. L. R.; Piso, T. R. C.; van der Heide, N. J.; Galenkamp, N. S.; Hermans, J.; Wloka, C.; Maglia, G. Automated electrical quantification of vitamin B1 in a bodily fluid using an engineered nanopore sensor. *Angew. Chem., Int. Ed.* **2021**, *60*, 22849–22855.

[22] Huang, G.; Voet, A.; Maglia, G. FraC nanopores with adjustable diameter identify the mass of opposite-charge peptides with 44 Dalton resolution. *Nat. Commun.* **2019**, *10*, 835.

[23] Liu, W.; Zhu, Q.; Yang, C. N.; Fu, Y. H.; Zhang, J. C.; Li, M. Y.; Yang, Z. L.; Xin, K. L.; Ma, J.; Winterhalter, M. et al. Single-molecule sensing inside stereo-and regio-defined hetero-nanopores. *Nat. Nanotechnol.* **2024**, *19*, 1693–1701.

[24] Wu, X. Y.; Li, M. Y.; Yang, S. J.; Jiang, J.; Ying, Y. L.; Chen, P. R.; Long, Y. T. Controlled genetic encoding of unnatural amino acids in a protein nanopore. *Angew. Chem., Int. Ed.* **2023**, *62*, e202300582.

[25] Qing, Y.; Ionescu, S. A.; Pulcu, G. S.; Bayley, H. Directional control of a processive molecular hopper. *Science* **2018**, *361*, 908–912.

[26] Rojko, N.; Dalla Serra, M.; Maček, P.; Anderluh, G. Pore formation by actinoporins, cytolysins from sea anemones. *Biochim. Biophys. Acta-Biomembr.* **2016**, *1858*, 446–456.

[27] Ulhuq, F. R.; Mariano, G. Bacterial pore-forming toxins. *Microbiology* **2022**, *168*, 001154.

[28] Anton, J. S.; Iacovache, I.; Bada Juarez, J. F.; Abriata, L. A.; Perrin, L. W.; Cao, C.; Marcaida, M. J.; Zuber, B.; Dal Peraro, M. Aerolysin nanopore structures revealed at high resolution in a lipid environment. *J. Am. Chem. Soc.* **2025**, *147*, 4984–4992.

[29] Vreeker, E.; Grünewald, F.; van der Heide, N. J.; Bonini, A.;

Marrink, S. J.; Tych, K. K.; Maglia, G. Nanopore-functionalized hybrid lipid-block copolymer membranes allow efficient single-molecule sampling and stable sensing of human serum. *Adv. Mater.* **2025**, *37*, 2418462.

[30] Zhao, C. J.; Wang, Y.; Chen, C.; Zhu, Y. B.; Miao, Z.; Mou, X. Y.; Yuan, W. D.; Zhang, Z. H.; Li, K. J.; Chen, M. T. et al. Direct and continuous monitoring of multicomponent antibiotic gentamicin in blood at single-molecule resolution. *ACS Nano* **2024**, *18*, 9137–9149.

[31] Lee, K.; Park, K. B.; Kim, H. J.; Yu, J. S.; Chae, H.; Kim, H. M.; Kim, K. B. Recent progress in solid-state nanopores. *Adv. Mater.* **2018**, *30*, 1704680.

[32] Ding, D. F.; Gao, P. C.; Ma, Q.; Wang, D. G.; Xia, F. Biomolecule-functionalized solid-state ion nanochannels/nanopores: Features and techniques. *Small* **2019**, *15*, 1804878.

[33] Pérez-Mitta, G.; Toimil-Molares, M. E.; Trautmann, C.; Marmisollé, W. A.; Azzaroni, O. Molecular design of solid-state nanopores: Fundamental concepts and applications. *Adv. Mater.* **2019**, *31*, 1901483.

[34] Cairns-Gibson, D. F.; Cockroft, S. L. Functionalised nanopores: Chemical and biological modifications. *Chem. Sci.* **2022**, *13*, 1869–1882.

[35] Ying, Y. L.; Hu, Z. L.; Zhang, S. L.; Qing, Y.; Fragasso, A.; Maglia, G.; Meller, A.; Bayley, H.; Dekker, C.; Long, Y. T. Nanopore-based technologies beyond DNA sequencing. *Nat. Nanotechnol.* **2022**, *17*, 1136–1146.

[36] Cao, C.; Long, Y. T. Biological nanopores: Confined spaces for electrochemical single-molecule analysis. *Acc. Chem. Res.* **2018**, *51*, 331–341.

[37] Pavlenok, M.; Derrington, I. M.; Gundlach, J. H.; Niederweis, M. MspA nanopores from subunit dimers. *PLoS One* **2012**, *7*, e38726.

[38] Scott, A. J.; Niitsu, A.; Kratochvil, H. T.; Lang, E. J. M.; Sengel, J. T.; Dawson, W. M.; Mahendran, K. R.; Mravic, M.; Thomson, A. R.; Brady, R. L. et al. Constructing ion channels from water-soluble α-helical barrels. *Nat. Chem.* **2021**, *13*, 643–650.

[39] Xu, C. F.; Lu, P. L.; Gamal El-Din, T. M.; Pei, X. Y.; Johnson, M. C.; Uyeda, A.; Bick, M. J.; Xu, Q.; Jiang, D. H.; Bai, H. et al. Computational design of transmembrane pores. *Nature* **2020**, *585*, 129–134.

[40] Huang, G.; Willems, K.; Soskine, M.; Wloka, C.; Maglia, G. Electro-osmotic capture and ionic discrimination of peptide and protein biomarkers with FraC nanopores. *Nat. Commun.* **2017**, *8*, 935.

[41] Restrepo-Pérez, L.; Wong, C. H.; Maglia, G.; Dekker, C.; Joo, C. Label-free detection of post-translational modifications with a nanopore. *Nano Lett.* **2019**, *19*, 7957–7964.

[42] Wei, X.; Wen, J. Q.; Wu, H.; Qu, Z. B.; Huang, G. Obtaining narrow distributions of single-molecule peptide signals enables sensitive peptide discrimination with α-hemolysin nanopores. *J. Am. Chem. Soc.* **2025**, *147*, 9304–9315.

[43] Sauciuc, A.; Morozzo della Rocca, B.; Tadema, M. J.; Chinappi, M.; Maglia, G. Translocation of linearized full-length proteins through an engineered nanopore under opposing electrophoretic force. *Nat. Biotechnol.* **2024**, *42*, 1275–1281.

[44] Versloot, R. C. A.; Straathof, S. A. P.; Stouwie, G.; Tadema, M. J.; Maglia, G. β-barrel nanopores with an acidic-aromatic sensing region identify proteinogenic peptides at low pH. *ACS Nano* **2022**, *16*, 7258–7268.

[45] Sauciuc, A.; Maglia, G. Controlled translocation of proteins through a biological nanopore for single-protein fingerprint identification. *Nano Lett.* **2024**, *24*, 14118–14124.

[46] Foster, J. C.; Pham, B.; Pham, R.; Kim, M.; Moore, M. D.; Chen, M. An engineered OmpG nanopore with displayed peptide motifs for single-molecule multiplex protein detection. *Angew. Chem., Int. Ed.* **2023**, *62*, e202214566.

[47] Zhang, X. L.; Galenkamp, N. S.; van der Heide, N. J.; Moreno, J.; Maglia, G.; Kjems, J. Specific detection of proteins by a nanobody-functionalized nanopore sensor. *ACS Nano* **2023**, *17*, 9167–9177.

[48] Movileanu, L.; Howorka, S.; Braha, O.; Bayley, H. Detecting protein analytes that modulate transmembrane movement of a polymer chain within a single protein pore. *Nat. Biotechnol.* **2000**, *18*, 1091–1095.

[49] Megalathan, A.; Cox, B. D.; Wilkerson, P. D.; Kaur, A.; Sapkota, K.; Reiner, J. E.; Dhakal, S. Single-molecule analysis of I-motif within self-assembled DNA duplexes and nanocircles. *Nucleic Acids Res.* **2019**, *47*, 7199–7212.

[50] Lee, Y.; Chong, S.; Lee, C.; Kim, J.; Choi, S. Q. Structural determinants of chirally selective transport of amino acids through the α-hemolysin protein nanopores of free-standing planar lipid membranes. *Nano Lett.* **2024**, *24*, 681–687.

[51] Du, X. Y.; Zhang, S. Y.; Wang, L. Y.; Wang, Y. Q.; Fan, P. P.; Jia, W. D.; Zhang, P. K.; Huang, S. Single-molecule interconversion between chiral configurations of boronate esters observed in a nanoreactor. *ACS Nano* **2023**, *17*, 2881–2892.

[52] Galenkamp, N. S.; Biesemans, A.; Maglia, G. Directional conformer exchange in dihydrofolate reductase revealed by single-molecule nanopore recordings. *Nat. Chem.* **2020**, *12*, 481–488.

[53] Qing, Y.; Bayley, H. Enzymeless DNA base identification by chemical stepping in a nanopore. *J. Am. Chem. Soc.* **2021**, *143*, 18181–18187.

[54] Qing, Y.; Tamagaki-Asahina, H.; Ionescu, S. A.; Liu, M. D.; Bayley, H. Catalytic site-selective substrate processing within a tubular nanoreactor. *Nat. Nanotechnol.* **2019**, *14*, 1135–1142.

[55] Zhang, M.; Tang, C.; Wang, Z. C.; Chen, S. C.; Zhang, D.; Li, K. J.; Sun, K.; Zhao, C. J.; Wang, Y.; Xu, M. Y. et al. Real-time detection of 20 amino acids and discrimination of pathologically relevant peptides with functionalized nanopore. *Nat. Methods* **2024**, *21*, 609–618.

[56] Wang, K. F.; Zhang, S. Y.; Zhou, X.; Yang, X.; Li, X. Y.; Wang, Y. Q.; Fan, P. P.; Xiao, Y. Q.; Sun, W.; Zhang, P. K. et al. Unambiguous discrimination of all 20 proteinogenic amino acids and their modifications by nanopore. *Nat. Methods* **2024**, *21*, 92–101.

[57] Zhang, Y.; Yi, Y. K.; Li, Z. Y.; Zhou, K.; Liu, L.; Wu, H. C. Peptide sequencing based on host-guest interaction-assisted nanopore sensing. *Nat. Methods* **2024**, *21*, 102–109.

[58] Li, Z. Y.; Yi, Y. K.; Zhang, Y.; Xiao, Y. Y.; Ren, Q. Y.; Zhou, K.; Liu, L.; Wu, H. C. Nanopore-based high-resolution detection of multiple post-translational modifications in protein. *Angew. Chem., Int. Ed.* **2025**, *64*, e202423801.

[59] Howorka, S.; Siwy, Z. S. Reading amino acids in a nanopore. *Nat. Biotechnol.* **2020**, *38*, 159–160.

[60] Lu, C. Z.; Bonini, A.; Viel, J. H.; Maglia, G. Toward single-molecule protein sequencing using nanopores. *Nat. Biotechnol.* **2025**, *43*, 312–322.

[61] Wei, X. J.; Penkauskas, T.; Reiner, J. E.; Kennard, C.; Uline, M. J.; Wang, Q.; Li, S.; Aksimentiev, A.; Robertson, J. W. F.; Liu, C. Engineering biological nanopore approaches toward protein sequencing. *ACS Nano* **2023**, *17*, 16369–16395.

[62] Zhang, S. L.; Huang, G.; Versloot, R. C. A.; Bruininks, B. M. H.; de Souza, P. C. T.; Marrink, S. J.; Maglia, G. Bottom-up fabrication of a proteasome-nanopore that unravels and processes single proteins. *Nat. Chem.* **2021**, *13*, 1192–1199.

[63] Wang, S. Y.; Zhao, Z. Y.; Haque, F.; Guo, P. X. Engineering of protein nanopores for sequencing, chemical or protein sensing and disease diagnosis. *Curr. Opin. Biotechnol.* **2018**, *51*, 80–89.

[64] Arora, P.; Zheng, H. Y.; Munusamy, S.; Jahani, R.; Wang, L.; Guan, X. Y. Probe-assisted detection of Fe^{3+} ions in a multi-functionalized nanopore. *Biosens. Bioelectron.* **2024**, *251*, 116125.

[65] Kang, X. F.; Cheley, S.; Rice-Ficht, A. C.; Bayley, H. A storable encapsulated bilayer chip containing a single protein nanopore. *J. Am. Chem. Soc.* **2007**, *129*, 4701–4705.

[66] Chen, X. H.; Zhang, Y. W.; Arora, P.; Guan, X. Y. Nanopore stochastic sensing based on non-covalent interactions. *Anal. Chem.* **2021**, *93*, 10974–10981.

[67] Cheley, S.; Gu, L. Q.; Bayley, H. Stochastic sensing of nanomolar inositol 1,4,5-trisphosphate with an engineered pore. *Chem. Biol.* **2002**, *9*, 829–838.

[68] Tian, L.; Wang, Y.; Kang, X. F. Target-controlled liposome amplification for versatile nanopore analysis. *Chem. Commun.* **2019**, *55*, 5159–5162.

[69] Xia, B. Q.; Fang, J.; Ma, S. Z.; Ma, M. Y.; Yao, G. D.; Li, T. H.; Cheng, X.; Wen, L. Q.; Gao, Z. B. Mapping the acetylamino and carboxyl groups on glycans by engineered α-hemolysin nanopores. *J. Am. Chem. Soc.* **2023**, *145*, 18812–18824.

[70] Yao, G. D.; Tian, Y. P.; Ke, W. J.; Fang, J.; Ma, S. Z.; Li, T. H.; Cheng, X.; Xia, B. Q.; Wen, L. Q.; Gao, Z. B. Direct identification of complex glycans via a highly sensitive engineered nanopore. *J. Am. Chem. Soc.* **2024**, *146*, 13356–13366.

[71] Cracknell, J. A.; Japrung, D.; Bayley, H. Translocating kilobase RNA through the staphylococcal α-hemolysin nanopore. *Nano Lett.* **2013**, *13*, 2500–2505.

[72] Maglia, G.; Henricus, M.; Wyss, R.; Li, Q. H.; Cheley, S.; Bayley, H. DNA strands from denatured duplexes are translocated through engineered protein nanopores at alkaline pH. *Nano Lett.* **2009**, *9*, 3831–3836.

[73] Jiang, J.; Li, M. Y.; Wu, X. Y.; Ying, Y. L.; Han, H. X.; Long, Y. T. Protein nanopore reveals the renin-angiotensin system crosstalk with single-amino-acid resolution. *Nat. Chem.* **2023**, *15*, 578–586.

[74] Huo, M. Z.; Li, M. Y.; Ying, Y. L.; Long, Y. T. Is the volume exclusion model practicable for nanopore protein sequencing. *Anal. Chem.* **2021**, *93*, 11364–11369.

[75] Huo, M. Z.; Hu, Z. L.; Ying, Y. L.; Long, Y. T. Enhanced identification of Tau acetylation and phosphorylation with an engineered aerolysin nanopore. *Proteomics* **2022**, *22*, 2100041.

[76] Lu, W. Q.; Zhao, X. J.; Li, M. M.; Li, Y. T.; Zhang, C.; Xiong, Y. T.; Li, J. Q.; Zhou, H.; Ye, X. L.; Li, X. N. et al. Precise structural analysis of neutral glycans using aerolysin mutant T240R nanopore. *ACS Nano* **2024**, *18*, 12412–12426.

[77] Bhatti, H.; Jawed, R.; Liu, H.; Ali, I.; Zhu, L. B.; Liu, Q. J. Clear discrimination of single-molecule of a single-stranded DNA homopolymers and hetero-homopolymers through a new mutant of *Mycobacterium smegmatis* porin A, MspA. *Nanosci. Nanotechnol. Lett.* **2019**, *11*, 1104–1115.

[78] Butler, T. Z.; Pavlenok, M.; Derrington, I. M.; Niederweis, M.; Gundlach, J. H. Single-molecule DNA detection with an engineered MspA protein nanopore. *Proc. Natl. Acad. Sci. USA* **2008**, *105*, 20647–20652.

[79] Manrao, E. A.; Derrington, I. M.; Pavlenok, M.; Niederweis, M.; Gundlach, J. H. Nucleotide discrimination with DNA immobilized in the MSPA nanopore. *PLoS One* **2011**, *6*, e25723.

[80] Brinkerhoff, H.; Kang, A. S. W.; Liu, J. Q.; Aksimentiev, A.; Dekker, C. Multiple rereads of single proteins at single-amino acid resolution using nanopores. *Science* **2021**, *374*, 1509–1513.

[81] Thomas, C. A.; Craig, J. M.; Hoshika, S.; Brinkerhoff, H.; Huang, J. R.; Abell, S. J.; Kim, H. C.; Franzi, M. C.; Carrasco, J. D.; Kim, H. J. et al. Assessing readability of an 8-letter expanded deoxyribonucleic acid alphabet with nanopores. *J. Am. Chem. Soc.* **2023**, *145*, 8560–8568.

[82] Chen, Z. J.; Wang, Z. Q.; Xu, Y.; Zhang, X. C.; Tian, B. X.; Bai, J. W. Controlled movement of ssDNA conjugated peptide through *Mycobacterium smegmatis* porin A (MspA) nanopore by a helicase motor for peptide sequencing application. *Chem. Sci.* **2021**, *12*, 15750–15756.

[83] Laszlo, A. H.; Craig, J. M.; Gavrilov, M.; Tippana, R.; Nova, I. C.; Huang, J. R.; Kim, H. C.; Abell, S. J.; DeCampos-Stairiker, M.; Mount, J. W. et al. Sequence-dependent mechanochemical coupling of helicase translocation and unwinding at single-nucleotide resolution. *Proc. Natl. Acad. Sci. USA* **2022**, *119*, e2202489119.

[84] Marx, S. K.; Mickolajczyk, K. J.; Craig, J. M.; Thomas, C. A.; Pfeffer, A. M.; Abell, S. J.; Carrasco, J. D.; Franzi, M. C.; Huang, J. R.; Kim, H. C. et al. Observing inhibition of the SARS-CoV-2 helicase at single-nucleotide resolution. *Nucleic Acids Res.* **2023**, *51*, 9266–9278.

[85] Derrington, I. M.; Craig, J. M.; Stava, E.; Laszlo, A. H.; Ross, B. C.; Brinkerhoff, H.; Nova, I. C.; Doering, K.; Tickman, B. I.; Ronaghi, M. et al. Subangstrom single-molecule measurements of motor proteins using a nanopore. *Nat. Biotechnol.* **2015**, *33*, 1073–1075.

[86] Wang, Y.; Patil, K. M.; Yan, S. H.; Zhang, P. K.; Guo, W. M.; Wang, Y. Q.; Chen, H. Y.; Gillingham, D.; Huang, S. Nanopore sequencing accurately identifies the mutagenic DNA lesion O^6-carboxymethyl guanine and reveals its behavior in replication. *Angew. Chem., Int. Ed.* **2019**, *58*, 8432–8436.

[87] Laszlo, A. H.; Derrington, I. M.; Brinkerhoff, H.; Langford, K. W.; Nova, I. C.; Samson, J. M.; Bartlett, J. J.; Pavlenok, M.; Gundlach, J. H. Detection and mapping of 5-methylcytosine and 5-hydroxymethylcytosine with nanopore MspA. *Proc. Natl. Acad. Sci. USA* **2013**, *110*, 18904–18909.

[88] Craig, J. M.; Laszlo, A. H.; Derrington, I. M.; Ross, B. C.; Brinkerhoff, H.; Nova, I. C.; Doering, K.; Tickman, B. I.; Svet, M. T.; Gundlach, J. H. Direct detection of unnatural DNA nucleotides dNaM and d5SICS using the MspA nanopore. *PLoS One* **2015**, *10*, e0143253.

[89] Yan, S. H.; Zhang, J. Y.; Wang, Y.; Guo, W. M.; Zhang, S. Y.; Liu, Y.; Cao, J.; Wang, Y. Q.; Wang, L. Y.; Ma, F. B. et al. Single molecule ratcheting motion of peptides in a *Mycobacterium smegmatis* porin A (MspA) nanopore. *Nano Lett.* **2021**, *21*, 6703–6710.

[90] Sun, K.; Ju, Y.; Chen, C.; Zhang, P.; Sawyer, E.; Luo, Y. F.; Geng, J. Single-molecule interaction of peptides with a biological nanopore for identification of protease activity. *Small Methods* **2020**, *4*, 1900892.

[91] Liu, Y.; Pan, T. Z.; Wang, K. F.; Wang, Y. Q.; Yan, S. H.; Wang, L. Y.; Zhang, S. Y.; Du, X. Y.; Jia, W. D.; Zhang, P. K. et al. Allosteric switching of calmodulin in a *Mycobacterium smegmatis* porin A (MspA) nanopore-trap. *Angew. Chem., Int. Ed.* **2021**, *60*, 23863–23870.

[92] Chingarande, R. G.; Tian, K.; Kuang, Y.; Sarangee, A.; Hou, C. R.; Ma, E.; Ren, J.; Hawkins, S.; Kim, J.; Adelstein, R. et al. Real-time label-free detection of dynamic aptamer-small molecule interactions using a nanopore nucleic acid conformational sensor. *Proc. Natl. Acad. Sci. USA* **2023**, *120*, e2108118120.

[93] Liu, Y.; Wang, K. F.; Wang, Y. Q.; Wang, L. Y.; Yan, S. H.; Du, X. Y.; Zhang, P. K.; Chen, H. Y.; Huang, S. Machine learning assisted simultaneous structural profiling of differently charged proteins in a *Mycobacterium smegmatis* porin A (MspA) electroosmotic trap. *J. Am. Chem. Soc.* **2022**, *144*, 757–768.

[94] Wang, Y. Q.; Li, M. Y.; Qiu, H.; Cao, C.; Wang, M. B.; Wu, X. Y.; Huang, J.; Ying, Y. L.; Long, Y. T. Identification of essential sensitive regions of the aerolysin nanopore for single oligonucleotide analysis. *Anal. Chem.* **2018**, *90*, 7790–7794.

[95] Li, M. Y.; Wang, Y. Q.; Lu, Y.; Ying, Y. L.; Long, Y. T. Single molecule study of hydrogen bond interactions between single oligonucleotide and aerolysin sensing interface. *Front. Chem.* **2019**, *7*, 528.

[96] Li, M. Y.; Ying, Y. L.; Li, S.; Wang, Y. Q.; Wu, X. Y.; Long, Y. T. Unveiling the heterogenous dephosphorylation of DNA using an aerolysin nanopore. *ACS Nano* **2020**, *14*, 12571–12578.

[97] Li, M. Y.; Wang, Y. Q.; Ying, Y. L.; Long, Y. T. Revealing the transient conformations of a single flavin adenine dinucleotide using an aerolysin nanopore. *Chem. Sci.* **2019**, *10*, 10400–10404.

[98] Li, M. Y.; Niu, H. Y.; Jiang, J.; Wu, X. Y.; Ying, Y. L.; Long, Y. T. Real-time recording the dynamic catalytic heterogeneity of enzymatic reactions using a nanopore. *J. Am. Chem. Soc.* **2025**, *147*, 17121–17131.

[99] Zhao, Q. T.; Jayawardhana, D. A.; Wang, D. Q.; Guan, X. Y. Study of peptide transport through engineered protein channels. *J. Phys. Chem. B* **2009**, *113*, 3572–3578.

[100] Roozbahani, G. M.; Chen, X. H.; Zhang, Y. W.; Xie, R. Q.; Ma, R.; Li, D. E.; Li, H. Z.; Guan, X. Y. Peptide-mediated nanopore detection of uranyl ions in aqueous media. *ACS Sens.* **2017**, *2*, 703–709.
[101] Wang, L.; Han, Y. J.; Zhou, S.; Guan, X. Y. Real-time label-free measurement of HIV-1 protease activity by nanopore analysis. *Biosens. Bioelectron.* **2014**, *62*, 158–162.
[102] Zhou, S.; Wang, L.; Chen, X. H.; Guan, X. Y. Label-free nanopore single-molecule measurement of trypsin activity. *ACS Sens.* **2016**, *1*, 607–613.
[103] Lucas, F. L. R.; Versloot, R. C. A.; Yakovlieva, L.; Walvoort, M. T. C.; Maglia, G. Protein identification by nanopore peptide profiling. *Nat. Commun.* **2021**, *12*, 5795.
[104] Versloot, R. C. A.; Lucas, F. L. R.; Yakovlieva, L.; Tadema, M. J.; Zhang, Y. R.; Wood, T. M.; Martin, N. I.; Marrink, S. J.; Walvoort, M. T. C.; Maglia, G. Quantification of protein glycosylation using nanopores. *Nano Lett.* **2022**, *22*, 5357–5364.
[105] Niu, H. Y.; Li, M. Y.; Ying, Y. L.; Long, Y. T. An engineered third electrostatic constriction of aerolysin to manipulate heterogeneously charged peptide transport. *Chem. Sci.* **2022**, *13*, 2456–2461.
[106] Cao, C.; Krapp, L. F.; Al Ouahabi, A.; König, N. F.; Cirauqui, N.; Radenovic, A.; Lutz, J. F.; Dal Peraro, M. Aerolysin nanopores decode digital information stored in tailored macromolecular analytes. *Sci. Adv.* **2020**, *6*, eabc2661.
[107] Camazzola, A.; Buglakova, E.; Perrin, L. W.; Rukes, V.; Cao, C. Eliminating the interference of neighboring nucleobases in aerolysin for nanopore sequencing. *ACS Sens.* **2025**, *10*, 4202–4208.
[108] Chang, J. W.; Gao, Y.; Zou, A. H.; Li, M. Y.; Long, Y. T.; Jiang, J. Precise identification of native peptides with posttranslational proline hydroxylation by nanopore. *Angew. Chem., Int. Ed.* **2025**, *64*, e202422692.
[109] Bikwemu, R.; Wolfe, A. J.; Xing, X. J.; Movileanu, L. Facilitated translocation of polypeptides through a single nanopore. *J. Phys.: Condens. Matter* **2010**, *22*, 454117.
[110] Mohammad, M. M.; Prakash, S.; Matouschek, A.; Movileanu, L. Controlling a single protein in a nanopore through electrostatic traps. *J. Am. Chem. Soc.* **2008**, *130*, 4081–4088.
[111] Movileanu, L. Squeezing a single polypeptide through a nanopore. *Soft Matter.* **2008**, *4*, 925–931.
[112] Gu, L. Q.; Cheley, S.; Bayley, H. Electroosmotic enhancement of the binding of a neutral molecule to a transmembrane pore. *Proc. Natl. Acad. Sci. USA* **2003**, *100*, 15498–15503.
[113] Martin-Baniandres, P.; Lan, W. H.; Board, S.; Romero-Ruiz, M.; Garcia-Manyes, S.; Qing, Y.; Bayley, H. Enzyme-less nanopore detection of post-translational modifications within long polypeptides. *Nat. Nanotechnol.* **2023**, *18*, 1335–1340.
[114] Franceschini, L.; Mikhailova, E.; Bayley, H.; Maglia, G. Nucleobase recognition at alkaline pH and apparent pK_a of single DNA bases immobilised within a biological nanopore. *Chem. Commun.* **2012**, *48*, 1520–1522.
[115] Wallace, E. V. B.; Stoddart, D.; Heron, A. J.; Mikhailova, E.; Maglia, G.; Donohoe, T. J.; Bayley, H. Identification of epigenetic DNA modifications with a protein nanopore. *Chem. Commun.* **2010**, *46*, 8195–8197.
[116] Ayub, M.; Bayley, H. Individual RNA base recognition in immobilized oligonucleotides using a protein nanopore. *Nano Lett.* **2012**, *12*, 5637–5643.
[117] Stoddart, D.; Maglia, G.; Mikhailova, E.; Heron, A. J.; Bayley, H. Multiple base-recognition sites in a biological nanopore: Two heads are better than one. *Angew. Chem., Int. Ed.* **2010**, *49*, 556–559.
[118] Li, S.; Wu, X. Y.; Li, M. Y.; Liu, S. C.; Ying, Y. L.; Long, Y. T. T232K/K238Q aerolysin nanopore for mapping adjacent phosphorylation sites of a single Tau peptide. *Small Methods* **2020**, *4*, 2000014.
[119] Fu, Y. H.; Li, X. Y.; Ma, L. Y.; Wan, Y. J.; Zhang, L. M.; Ying, Y. L.; Long, Y. T. Exploring the single-molecule transient interactions with nanopore frequency spectrum. *J. Phys. Chem. C* **2024**, *128*, 1110–1115.
[120] Wu, H. C.; Bayley, H. Single-molecule detection of nitrogen mustards by covalent reaction within a protein nanopore. *J. Am. Chem. Soc.* **2008**, *130*, 6813–6819.
[121] Pulcu, G. S.; Mikhailova, E.; Choi, L. S.; Bayley, H. Continuous observation of the stochastic motion of an individual small-molecule walker. *Nat. Nanotechnol.* **2015**, *10*, 76–83.
[122] Zhou, B.; Wang, Y. Q.; Cao, C.; Li, D. W.; Long, Y. T. Monitoring disulfide bonds making and breaking in biological nanopore at single molecule level. *Sci. China Chem.* **2018**, *61*, 1385–1388.
[123] Liu, W.; Yang, C. N.; Yang, Z. L.; Yu, R. J.; Long, Y. T.; Ying, Y. L. Observing confined local oxygen-induced reversible thiol/disulfide cycle with a protein nanopore. *Angew. Chem., Int. Ed.* **2023**, *62*, e202304023.
[124] Li, F. J.; Foster, J. C.; Nguyen, L.; Chen, M. Selective identification of allosteric inhibitors and co-drug combinations targeting kinases by using a nanopore tweezer approach. *ACS Nano* **2025**, *19*, 34617–34627.
[125] Liu, W.; Yang, Z. L.; Yang, C. N.; Ying, Y. L.; Long, Y. T. Profiling single-molecule reaction kinetics under nanopore confinement. *Chem. Sci.* **2022**, *13*, 4109–4114.
[126] Yang, C. N.; Liu, W.; Liu, H. T.; Zhang, J. C.; Long, Y. T.; Ying, Y. L. Electrochemical kinetic fingerprinting of single-molecule coordinations in confined nanopores. *Faraday Discuss.* **2025**, *257*, 29–43.
[127] Cao, J.; Jia, W. D.; Zhang, J. Y.; Xu, X. M.; Yan, S. H.; Wang, Y. Q.; Zhang, P. K.; Chen, H. Y.; Huang, S. Giant single molecule chemistry events observed from a tetrachloroaurate(III) embedded *Mycobacterium smegmatis* porin A nanopore. *Nat. Commun.* **2019**, *10*, 5668.
[128] Cao, J.; Zhang, S. Y.; Zhang, J. Y.; Wang, S.; Jia, W. D.; Yan, S. H.; Wang, Y. Q.; Zhang, P. K.; Chen, H. Y.; Huang, S. A single-molecule observation of dichloroaurate(I) binding to an engineered *Mycobacterium smegmatis* porin A (MspA) nanopore. *Anal. Chem.* **2021**, *93*, 1529–1536.
[129] Maglia, G.; Restrepo, M. R.; Mikhailova, E.; Bayley, H. Enhanced translocation of single DNA molecules through α-hemolysin nanopores by manipulation of internal charge. *Proc. Natl. Acad. Sci. USA* **2008**, *105*, 19720–19725.
[130] Campos, E.; Asandei, A.; McVey, C. E.; Dias, J. C.; Oliveira, A. S. F.; Soares, C. M.; Luchian, T.; Astier, Y. The role of Lys147 in the interaction between MPSA-gold nanoparticles and the α-hemolysin nanopore. *Langmuir* **2012**, *28*, 15643–15650.
[131] Campos, E.; McVey, C. E.; Carney, R. P.; Stellacci, F.; Astier, Y.; Yates, J. Sensing single mixed-monolayer protected gold nanoparticles by the α-hemolysin nanopore. *Anal. Chem.* **2013**, *85*, 10149–10158.
[132] Franceschini, L.; Brouns, T.; Willems, K.; Carlon, E.; Maglia, G. DNA translocation through nanopores at physiological ionic strengths requires precise nanoscale engineering. *ACS Nano* **2016**, *10*, 8394–8402.
[133] Pham, B.; Chisholm, C. M.; Foster, J.; Friis, E.; Fahie, M. A.; Chen, M. A pH-independent quiet OmpG pore with enhanced electrostatic repulsion among the extracellular loops. *Biochim. Biophys. Acta-Biomembr.* **2021**, *1863*, 183485.
[134] Fahie, M. A. V.; Li, F. J.; Palmer, C.; Yoon, C.; Chen, M. Modifying the pH sensitivity of OmpG nanopore for improved detection at acidic pH. *Biophys. J.* **2022**, *121*, 731–741.
[135] von Rhein, C.; Bauer, S.; López Sanjurjo, E. J.; Benz, R.; Goebel, W.; Ludwig, A. ClyA cytolysin from *Salmonella*: Distribution within the genus, regulation of expression by SlyA, and pore-forming characteristics. *Int. J. Med. Microbiol.* **2009**, *299*, 21–35.
[136] Soskine, M.; Biesemans, A.; Moeyaert, B.; Cheley, S.; Bayley, H.; Maglia, G. An engineered ClyA nanopore detects folded target proteins by selective external association and pore entry. *Nano Lett.* **2012**, *12*, 4895–4900.
[137] Wloka, C.; Mutter, N. L.; Soskine, M.; Maglia, G. Alpha-helical Fragaceatoxin C nanopore engineered for double-stranded and single-

stranded nucleic acid analysis. *Angew. Chem., Int. Ed.* **2016**, *55*, 12494–12498.
[138] Van Meervelt, V.; Soskine, M.; Singh, S.; Schuurman-Wolters, G. K.; Wijma, H. J.; Poolman, B.; Maglia, G. Real-time conformational changes and controlled orientation of native proteins inside a protein nanoreactor. *J. Am. Chem. Soc.* **2017**, *139*, 18640–18646.
[139] Li, F. J.; Fahie, M. A.; Gilliam, K. M.; Pham, R.; Chen, M. Mapping the conformational energy landscape of Abl kinase using ClyA nanopore tweezers. *Nat. Commun.* **2022**, *13*, 3541.
[140] Van Meervelt, V.; Soskine, M.; Maglia, G. Detection of two isomeric binding configurations in a protein-aptamer complex with a biological nanopore. *ACS Nano* **2014**, *8*, 12826–12835.
[141] Galenkamp, N. S.; Maglia, G. Single-molecule sampling of dihydrofolate reductase shows kinetic pauses and an endosteric effect linked to catalysis. *ACS Catal.* **2022**, *12*, 1228–1236.
[142] Jeong, K. B.; Ryu, M.; Kim, J. S.; Kim, M.; Yoo, J.; Chung, M.; Oh, S.; Jo, G.; Lee, S. G.; Kim, H. M. et al. Single-molecule fingerprinting of protein-drug interaction using a funneled biological nanopore. *Nat. Commun.* **2023**, *14*, 1461.
[143] Ryu, M.; Oh, S.; Jeong, K. B.; Hwang, S.; Kim, J. S.; Chung, M.; Chi, S. W. Single-molecule-based, label-free monitoring of molecular glue efficacies for promoting protein-protein interactions using YaxAB nanopores. *ACS Nano* **2024**, *18*, 31451–31465.
[144] Braha, O.; Gu, L. Q.; Zhou, L.; Lu, X. F.; Cheley, S.; Bayley, H. Simultaneous stochastic sensing of divalent metal ions. *Nat. Biotechnol.* **2000**, *18*, 1005–1007.
[145] Gupta, J.; Zhao, Q. T.; Wang, G. H.; Kang, X. F.; Guan, X. Y. Simultaneous detection of CMPA and PMPA, hydrolytes of soman and cyclosarin nerve agents, by nanopore analysis. *Sens. Actuators B: Chem.* **2013**, *176*, 625–631.
[146] Clarke, J.; Wu, H. C.; Jayasinghe, L.; Patel, A.; Reid, S.; Bayley, H. Continuous base identification for single-molecule nanopore DNA sequencing. *Nat. Nanotechnol.* **2009**, *4*, 265–270.
[147] Qing, Y.; Pulcu, G. S.; Bell, N. A. W.; Bayley, H. Bioorthogonal cycloadditions with sub-millisecond intermediates. *Angew. Chem., Int. Ed.* **2018**, *57*, 1218–1221.
[148] Boersma, A. J.; Bayley, H. Continuous stochastic detection of amino acid enantiomers with a protein nanopore. *Angew. Chem., Int. Ed.* **2012**, *51*, 9606–9609.
[149] Zhang, S. Y.; Cao, Z. Y.; Fan, P. P.; Wang, Y. Q.; Jia, W. D.; Wang, L. Y.; Wang, K. F.; Liu, Y.; Du, X. Y.; Hu, C. Z. et al. A nanopore-based saccharide sensor. *Angew. Chem., Int. Ed.* **2022**, *61*, e202203769.
[150] Zhang, S. Y.; Cao, Z. Y.; Fan, P. P.; Sun, W.; Xiao, Y. Q.; Zhang, P. K.; Wang, Y. Q.; Huang, S. Discrimination of disaccharide isomers of different glycosidic linkages using a modified MspA nanopore. *Angew. Chem., Int. Ed.* **2024**, *63*, e202316766.
[151] Jiang, X. J.; Pan, T. Z.; Lang, C.; Zeng, C.; Hou, J. X.; Xu, J. Y.; Luo, Q.; Hou, C. X.; Liu, J. Q. Single-molecule observation of selenoenzyme intermediates in a semisynthetic seleno-α-hemolysin nanoreactor. *Anal. Chem.* **2022**, *94*, 8433–8440.
[152] Banerjee, A.; Mikhailova, E.; Cheley, S.; Gu, L. Q.; Montoya, M.; Nagaoka, Y.; Gouaux, E.; Bayley, H. Molecular bases of cyclodextrin adapter interactions with engineered protein nanopores. *Proc. Natl. Acad. Sci. USA* **2010**, *107*, 8165–8170.
[153] Cload, S. T.; Liu, D. R.; Froland, W. A.; Schultz, P. G. Development of improved tRNAs for *in vitro* biosynthesis of proteins containing unnatural amino acids. *Chem. Biol.* **1996**, *3*, 1033–1038.
[154] Yang, J.; Wang, K. F.; Zhang, S. Y.; Zheng, X. C.; Cui, T. X.; Yang, X.; Liu, Y.; Lu, D.; Wang, Y. Q.; Tian, X. et al. Site-specific introduction of bioorthogonal handles to nanopores by genetic code expansion. *Angew. Chem., Int. Ed.* **2023**, *62*, e202216115.
[155] Brabham, R.; Fascione, M. A. Pyrrolysine amber stop-codon suppression: Development and applications. *ChemBioChem* **2017**, *18*, 1973–1983.
[156] Lee, J.; Boersma, A. J.; Boudreau, M. A.; Cheley, S.; Daltrop, O.; Li, J. W.; Tamagaki, H.; Bayley, H. Semisynthetic nanoreactor for reversible single-molecule covalent chemistry. *ACS Nano* **2016**, *10*, 8843–8850.
[157] Lee, J.; Bayley, H. Semisynthetic protein nanoreactor for single-molecule chemistry. *Proc. Natl. Acad. Sci. USA* **2015**, *112*, 13768–13773.
[158] Gu, L. Q.; Braha, O.; Conlan, S.; Cheley, S.; Bayley, H. Stochastic sensing of organic analytes by a pore-forming protein containing a molecular adapter. *Nature* **1999**, *398*, 686–690.
[159] Gu, L. Q.; Cheley, S.; Bayley, H. Capture of a single molecule in a nanocavity. *Science* **2001**, *291*, 636–640.
[160] Gu, L. Q.; Cheley, S.; Bayley, H. Prolonged residence time of a noncovalent molecular adapter, β-cyclodextrin, within the lumen of mutant α-hemolysin pores. *J. Gen. Physiol.* **2001**, *118*, 481–494.
[161] Astier, Y.; Braha, O.; Bayley, H. Toward single molecule DNA sequencing: Direct identification of ribonucleoside and deoxyribonucleoside 5′-monophosphates by using an engineered protein nanopore equipped with a molecular adapter. *J. Am. Chem. Soc.* **2006**, *128*, 1705–1710.
[162] Li, M. J.; Rauf, A.; Guo, Y. L.; Kang, X. F. Real-time label-free kinetics monitoring of trypsin-catalyzed ester hydrolysis by a nanopore sensor. *ACS Sens.* **2019**, *4*, 2854–2857.
[163] Guo, Y. L.; Jian, F. F.; Kang, X. F. Nanopore sensor for copper ion detection using a polyamine decorated β-cyclodextrin as the recognition element. *RSC Adv.* **2017**, *7*, 15315–15320.
[164] Su, Z. Q.; Wei, Y. F.; Kang, X. F. Simultaneous high-resolution detection of bioenergetic molecules using biomimetic-receptor nanopore. *Anal. Chem.* **2019**, *91*, 15255–15259.
[165] Wei, Y. F.; Su, Z. Q.; Kang, X. F.; Guo, Y. L.; Mu, X. X. Single-molecule transformation and analysis of glutathione oxidized and reduced in nanopore. *Talanta* **2017**, *167*, 526–531.
[166] Zhuo, S.; Wang, Y.; Kang, X. F. Engineered protein nanopore for real-time monitoring single-molecule reaction between cadmium ion and glutathione. *Chin. J. Anal. Chem.* **2017**, *45*, 1172–1178.
[167] Liu, X. T.; Feng, W. Y.; Yao, F. J.; Zhang, J. L.; Ayesha, R.; Chen, T. T.; Shi, X. Y.; Qiao, X. X.; Ma, L. P.; Yu, S. et al. Biomimetic molecular clamp nanopores for simultaneous quantifications of NAD^+ and NADH. *Anal. Chem.* **2021**, *93*, 7118–7124.
[168] Wang, D. Q.; Zhao, Q. T.; Zoysa, R. S. S. D.; Guan, X. Y. Detection of nerve agent hydrolytes in an engineered nanopore. *Sens. Actuators B: Chem.* **2009**, *139*, 440–446.
[169] Cao, X. Y.; Guo, Y. L.; Feng, Y. H.; Liu, X. T.; Yao, F. J.; Chen, T. T.; Tian, L.; Kang, X. F. Recognition receptor for methylated arginine at the single molecular level. *Anal. Chem.* **2023**, *95*, 6989–6995.
[170] Guo, Y. L.; Niu, A. H.; Jian, F. F.; Wang, Y.; Yao, F. J.; Wei, Y. F.; Tian, L.; Kang, X. F. Metal-organic complex-functionalized protein nanopore sensor for aromatic amino acids chiral recognition. *Analyst* **2017**, *142*, 1048–1053.
[171] Kang, X. F.; Cheley, S.; Guan, X. Y.; Bayley, H. Stochastic detection of enantiomers. *J. Am. Chem. Soc.* **2006**, *128*, 10684–10685.
[172] Cui, R. K.; Wang, Z. Z.; Li, L. N.; Liu, L. L.; Li, Z.; Liu, X. T.; Chen, T. T.; Rauf, A.; Kang, X. F.; Guo, Y. L. Bionic nanopore recognition receptors for single-molecule enantioselectivity studies of chiral drugs. *Anal. Chim. Acta* **2024**, *1318*, 342960.
[173] Wu, H. C.; Astier, Y.; Maglia, G.; Mikhailova, E.; Bayley, H. Protein nanopores with covalently attached molecular adapters. *J. Am. Chem. Soc.* **2007**, *129*, 16142–16148.
[174] Chen, M.; Khalid, S.; Sansom, M. S. P.; Bayley, H. Outer membrane protein G: Engineering a quiet pore for biosensing. *Proc. Natl. Acad. Sci. USA* **2008**, *105*, 6272–6277.
[175] Duan, J.; Zhuo, S.; Yao, F. J.; Zhang, Y. N.; Kang, X. F. A single-molecule mycobacterium smegmatis porin A protein nanopore sensor for host-guest chemistry. *Chin. J. Anal. Chem.* **2016**, *44*, 1801–1807.
[176] Gurnev, P. A.; Harries, D.; Parsegian, V. A.; Bezrukov, S. M. The

dynamic side of the hofmeister effect: A single-molecule nanopore study of specific complex formation. *ChemPhysChem* **2009**, *10*, 1445–1449.

[177] Wei, X. J.; Choudhary, A.; Wang, L. Y.; Yang, L. X.; Uline, M. J.; Tagliazucchi, M.; Wang, Q.; Bedrov, D.; Liu, C. Single-molecule profiling of per- and polyfluoroalkyl substances by cyclodextrin mediated host-guest interactions within a biological nanopore. *Sci. Adv.* **2024**, *10*, eadp8134.

[178] Sanchez-Quesada, J.; Ghadiri, M. R.; Bayley, H.; Braha, O. Cyclic peptides as molecular adapters for a pore-forming protein. *J. Am. Chem. Soc.* **2000**, *122*, 11757–11766.

[179] Jiang, X. J.; Zang, M. S.; Li, F.; Hou, C. X.; Luo, Q.; Xu, J. Y.; Liu, J. Q. Highly sensitive detection of paraquat with pillar[5]arenes as an aptamer in an α-hemolysin nanopore. *Mater. Chem. Front.* **2021**, *5*, 7032–7040.

[180] Braha, O.; Webb, J.; Gu, L. Q.; Kim, K.; Bayley, H. Carriers versus adapters in stochastic sensing. *ChemPhysChem* **2005**, *6*, 889–892.

[181] Reany, O.; Romero-Ruiz, M.; Khurana, R.; Mondal, P.; Keinan, E.; Bayley, H. Stochastic sensing of chloride anions using an α-hemolysin pore with a *semiaza*-bambusuril adapter. *Angew. Chem., Int. Ed.* **2024**, *63*, e202406719.

[182] Ying, Y. L.; Zhang, J. J.; Meng, F. N.; Cao, C.; Yao, X. Y.; Willner, I.; Tian, H.; Long, Y. T. A stimuli-responsive nanopore based on a photoresponsive host-guest system. *Sci. Rep.* **2013**, *3*, 1662.

[183] Li, T.; Liu, L.; Li, Y. R.; Xie, J. N.; Wu, H. C. A universal strategy for aptamer-based nanopore sensing through host-guest interactions inside α-hemolysin. *Angew. Chem., Int. Ed.* **2015**, *54*, 7568–7571.

[184] Ren, Q. Y.; Hao, W. Y.; Wang, L. X.; Zhou, K.; Liu, L.; Wu, H. C. CH-π interactions elucidated at the single-molecule level. *J. Am. Chem. Soc.* **2025**, *147*, 34118–34125.

[185] Hao, W. Y.; Guo, B. Y.; Liu, J. C.; Ren, Q. Y.; Li, S. M.; Li, Q.; Zhou, K.; Liu, L.; Wu, H. C. Single-molecule exchange inside a nanocage provides insights into the origin of π-π interactions. *J. Am. Chem. Soc.* **2024**, *146*, 10206–10216.

[186] Boersma, A. J.; Brain, K. L.; Bayley, H. Real-time stochastic detection of multiple neurotransmitters with a protein nanopore. *ACS Nano* **2012**, *6*, 5304–5308.

[187] Ramsay, W. J.; Bayley, H. Single-molecule determination of the isomers of $_D$-glucose and $_D$-fructose that bind to boronic acids. *Angew. Chem., Int. Ed.* **2018**, *57*, 2841–2845.

[188] Liu, Y.; Zhang, S. Y.; Wang, Y. Q.; Wang, L. Y.; Cao, Z. Y.; Sun, W.; Fan, P. P.; Zhang, P. K.; Chen, H. Y.; Huang, S. Nanopore identification of alditol epimers and their application in rapid analysis of alditol-containing drinks and healthcare products. *J. Am. Chem. Soc.* **2022**, *144*, 13717–13728.

[189] Jia, W. D.; Ouyang, Y. S.; Zhang, S. Y.; Zhang, P. K.; Huang, S. Nanopore identification of L-, D-lactic acids, D-glucose and gluconic acid in the serum of human and animals. *Small Methods* **2025**, *9*, 2400664.

[190] Wang, K. F.; Yang, X.; Zhang, S. Y.; Zhang, P. K.; Huang, S. Nanopore discrimination of nucleotide sugars. *Nano Lett.* **2023**, *23*, 8620–8627.

[191] Wang, Y. Q.; Fan, P. P.; Zhang, S. Y.; Wang, L. Y.; Li, X. Y.; Jia, W. D.; Liu, Y.; Wang, K. F.; Du, X. Y.; Zhang, P. K. et al. Discrimination of ribonucleoside mono-, di-, and triphosphates using an engineered nanopore. *ACS Nano* **2022**, *16*, 21356–21365.

[192] Fan, P. P.; Li, K.; Li, T.; Zhang, P. K.; Huang, S. Nanopore signatures of major alcoholic beverages. *Matter* **2025**, *8*, 101931.

[193] Li, X. Y.; Wang, Y. Q.; Zhang, S. Y.; Zhang, P. K.; Huang, S. Nanopore identification of N-acetylation by hydroxylamine deacetylation (NINAHD). *ACS Sens.* **2024**, *9*, 1359–1371.

[194] Ouyang, Y. S.; Wang, K. F.; Jia, W. D.; Zhang, P. K.; Huang, S. Simultaneous identification of vitamins B1, B3, B5, and B6 by an engineered nanopore. *Nano Lett.* **2024**, *24*, 11944–11953.

[195] Sun, W.; Xiao, Y. Q.; Wang, K. F.; Zhang, S. Y.; Yao, L.; Li, T.; Cheng, B. X.; Zhang, P. K.; Huang, S. Nanopore discrimination of rare earth elements. *Nat. Nanotechnol.* **2025**, *20*, 523–531.

[196] Wang, J. J.; Bafna, J. A.; Bhamidimarri, S. P.; Winterhalter, M. Small-molecule permeation across membrane channels: Chemical modification to quantify transport across OmpF. *Angew. Chem., Int. Ed.* **2019**, *58*, 4737–4741.

[197] Kahlstatt, J.; Reiß, P.; Halbritter, T.; Essen, L. O.; Koert, U.; Heckel, A. A light-triggered transmembrane porin. *Chem. Commun.* **2018**, *54*, 9623–9626.

[198] Chandramouli, B.; Di Maio, D.; Mancini, G.; Brancato, G. Introducing an artificial photo-switch into a biological pore: A model study of an engineered α-hemolysin. *Biochim. Biophys. Acta-Biomembr.* **2016**, *1858*, 689–697.

[199] Chang, C. Y.; Niblack, B.; Walker, B.; Bayley, H. A photogenerated pore-forming protein. *Chem. Biol.* **1995**, *2*, 391–400.

[200] Mutter, N. L.; Volarić, J.; Szymanski, W.; Feringa, B. L.; Maglia, G. Reversible photocontrolled nanopore assembly. *J. Am. Chem. Soc.* **2019**, *141*, 14356–14363.

[201] Zhuang, T. D.; Tamm, L. K. Control of the conductance of engineered protein nanopores through concerted loop motions. *Angew. Chem., Int. Ed.* **2014**, *53*, 5897–5902.

[202] Fan, Q. R.; Chen, H.; Wei, G. G.; Wei, D.; Wang, Z. K.; Zhang, L.; Wang, J.; Zhu, M. A review of conjugation technologies for antibody drug conjugates. *Antib. Ther.* **2025**, *8*, 157–170.

[203] Walsh, S. J.; Bargh, J. D.; Dannheim, F. M.; Hanby, A. R.; Seki, H.; Counsell, A. J.; Ou, X. X.; Fowler, E.; Ashman, N.; Takada, Y. et al. Site-selective modification strategies in antibody-drug conjugates. *Chem. Soc. Rev.* **2021**, *50*, 1305–1353.

[204] Deng, J. R.; Lai, N. C. H.; Kung, K. K. Y.; Yang, B.; Chung, S. F.; Leung, A. S. L.; Choi, M. C.; Leung, Y. C.; Wong, M. K. N-terminal selective modification of peptides and proteins using 2-ethynylbenzaldehydes. *Commun. Chem.* **2020**, *3*, 67.

[205] Li, B. X.; Kim, D. K.; Bloom, S.; Huang, R. Y. C.; Qiao, J. X.; Ewing, W. R.; Oblinsky, D. G.; Scholes, G. D.; MacMillan, D. W. C. Site-selective tyrosine bioconjugation via photoredox catalysis for native-to-bioorthogonal protein transformation. *Nat. Chem.* **2021**, *13*, 902–908.

[206] Taylor, M. T.; Nelson, J. E.; Suero, M. G.; Gaunt, M. J. A protein functionalization platform based on selective reactions at methionine residues. *Nature* **2018**, *562*, 563–568.

[207] Mohammad, M. M.; Iyer, R.; Howard, K. R.; McPike, M. P.; Borer, P. N.; Movileanu, L. Engineering a rigid protein tunnel for biomolecular detection. *J. Am. Chem. Soc.* **2012**, *134*, 9521–9531.

[208] Niedzwiecki, D. J.; Mohammad, M. M.; Movileanu, L. Inspection of the engineered FhuA Δc/Δ4L protein nanopore by polymer exclusion. *Biophys. J.* **2012**, *103*, 2115–2124.

[209] Tomita, N.; Mohammad, M. M.; Niedzwiecki, D. J.; Ohta, M.; Movileanu, L. Does the lipid environment impact the open-state conductance of an engineered β-barrel protein nanopore. *Biochim. Biophys. Acta-Biomembr.* **2013**, *1828*, 1057–1065.

[210] Liu, Z. Z.; Ghai, I.; Winterhalter, M.; Schwaneberg, U. Engineering enhanced pore sizes using FhuA Δ1-160 from *E. coli* outer membrane as template. *ACS Sens.* **2017**, *2*, 1619–1626.

[211] Thakur, A. K.; Larimi, M. G.; Gooden, K.; Movileanu, L. Aberrantly large single-channel conductance of polyhistidine arm-containing protein nanopores. *Biochemistry* **2017**, *56*, 4895–4905.

[212] Sanganna Gari, R. R.; Seelheim, P.; Liang, B. Y.; Tamm, L. K. Quiet outer membrane protein G (OmpG) nanopore for biosensing. *ACS Sens.* **2019**, *4*, 1230–1235.

[213] Bhamidimarri, S. P.; Prajapati, J. D.; van den Berg, B.; Winterhalter, M.; Kleinekathöfer, U. Role of electroosmosis in the permeation of neutral molecules: CymA and cyclodextrin as an example. *Biophys. J.* **2016**, *110*, 600–611.

[214] Prajapati, J. D.; Kleinekathöfer, U. Voltage-dependent transport of neutral solutes through nanopores: A molecular view. *J. Phys. Chem. B* **2020**, *124*, 10718–10731.

[215] Stoddart, D.; Ayub, M.; Höfler, L.; Raychaudhuri, P.; Klingelhoefer, J. W.; Maglia, G.; Heron, A.; Bayley, H. Functional truncated membrane pores. *Proc. Natl. Acad. Sci. USA* **2014**, *111*, 2425–2430.

[216] Ayub, M.; Stoddart, D.; Bayley, H. Nucleobase recognition by truncated α-hemolysin pores. *ACS Nano* **2015**, *9*, 7895–7903.
[217] Zhang, L.; Gardner, M. L.; Jayasinghe, L.; Jordan, M.; Aldana, J.; Burns, N.; Freitas, M. A.; Guo, P. X. Detection of single peptide with only one amino acid modification via electronic fingerprinting using reengineered durable channel of Phi29 DNA packaging motor. *Biomaterials* **2021**, *276*, 121022.
[218] Fahie, M. A.; Candido, J.; Andree, G.; Chen, M. Tuning protein discrimination through altering the sampling interface formed between the analyte and the OmpG nanopore. *ACS Sens.* **2021**, *6*, 1286–1294.
[219] Fahie, M.; Chisholm, C.; Chen, M. Resolved single-molecule detection of individual species within a mixture of *anti*-biotin antibodies using an engineered monomeric nanopore. *ACS Nano* **2015**, *9*, 1089–1098.
[220] Fahie, M. A.; Yang, B.; Mullis, M.; Holden, M. A.; Chen, M. Selective detection of protein homologues in serum using an OmpG nanopore. *Anal. Chem.* **2015**, *87*, 11143–11149.
[221] Fahie, M. A.; Chen, M. Electrostatic interactions between OmpG nanopore and analyte protein surface can distinguish between glycosylated isoforms. *J. Phys. Chem. B* **2015**, *119*, 10198–10206.
[222] Fahie, M. A.; Yang, B.; Pham, B.; Chen, M. Tuning the selectivity and sensitivity of an OmpG nanopore sensor by adjusting ligand tether length. *ACS Sens.* **2016**, *1*, 614–622.
[223] Howorka, S.; Cheley, S.; Bayley, H. Sequence-specific detection of individual DNA strands using engineered nanopores. *Nat. Biotechnol.* **2001**, *19*, 636–639.
[224] Howorka, S.; Movileanu, L.; Braha, O.; Bayley, H. Kinetics of duplex formation for individual DNA strands within a single protein nanopore. *Proc. Natl. Acad. Sci. USA* **2001**, *98*, 12996–13001.
[225] Howorka, S.; Bayley, H. Probing distance and electrical potential within a protein pore with tethered DNA. *Biophys. J.* **2002**, *83*, 3202–3210.
[226] Rotem, D.; Jayasinghe, L.; Salichou, M.; Bayley, H. Protein detection by nanopores equipped with aptamers. *J. Am. Chem. Soc.* **2012**, *134*, 2781–2787.
[227] Hwang, H. J.; Kim, J. S.; Lee, J.; Min, J. S.; Jeong, K. B.; Kim, E.; Lee, M. K.; Chi, S. W. Single-molecule sensing of an anticancer therapeutic protein-protein interaction using the chemically modified OmpG nanopore. *Anal. Chem.* **2022**, *94*, 7449–7454.
[228] Zhang, L.; Burns, N.; Ji, Z. X.; Sun, S.; Deutscher, S. L.; Carson III, W. E.; Guo, P. X. Nipple fluid for breast cancer diagnosis using the nanopore of Phi29 DNA-packaging motor. *Nanomedicine* **2023**, *48*, 102642.
[229] Zhang, L.; Burns, N.; Jordan, M.; Jayasinghe, L.; Guo, P. X. Macromolecule sensing and tumor biomarker detection by harnessing terminal size and hydrophobicity of viral DNA packaging motor channels into membranes and flow cells. *Biomater. Sci.* **2022**, *10*, 167–177.
[230] Wang, S. Y.; Haque, F.; Rychahou, P. G.; Evers, B. M.; Guo, P. X. Engineered nanopore of Phi29 DNA-packaging motor for real-time detection of single colon cancer specific antibody in serum. *ACS Nano* **2013**, *7*, 9814–9822.
[231] Cheley, S.; Xie, H. Z.; Bayley, H. A genetically encoded pore for the stochastic detection of a protein kinase. *ChemBioChem* **2006**, *7*, 1923–1927.
[232] Harrington, L.; Cheley, S.; Alexander, L. T.; Knapp, S.; Bayley, H. Stochastic detection of Pim protein kinases reveals electrostatically enhanced association of a peptide substrate. *Proc. Natl. Acad. Sci. USA* **2013**, *110*, E4417–26.
[233] Harrington, L.; Alexander, L. T.; Knapp, S.; Bayley, H. Pim kinase inhibitors evaluated with a single-molecule engineered nanopore sensor. *Angew. Chem., Int. Ed.* **2015**, *54*, 8154–8159.
[234] Harrington, L.; Alexander, L. T.; Knapp, S.; Bayley, H. Single-molecule protein phosphorylation and dephosphorylation by nanopore enzymology. *ACS Nano* **2019**, *13*, 633–641.
[235] Thakur, A. K.; Movileanu, L. Single-molecule protein detection in a biofluid using a quantitative nanopore sensor. *ACS Sens.* **2019**, *4*, 2320–2326.
[236] Sun, J. X.; Thakur, A. K.; Movileanu, L. Protein ligand-induced amplification in the 1/*f* noise of a protein-selective nanopore. *Langmuir* **2020**, *36*, 15247–15257.
[237] Thakur, A. K.; Movileanu, L. Real-time measurement of protein-protein interactions at single-molecule resolution using a biological nanopore. *Nat. Biotechnol.* **2019**, *37*, 96–101.
[238] Larimi, M. G.; Ha, J. H.; Loh, S. N.; Movileanu, L. Insertion state of modular protein nanopores into a membrane. *Biochim. Biophys. Acta-Biomembr.* **2021**, *1863*, 183570.
[239] Ahmad, M.; Ha, J. H.; Mayse, L. A.; Presti, M. F.; Wolfe, A. J.; Moody, K. J.; Loh, S. N.; Movileanu, L. A generalizable nanopore sensor for highly specific protein detection at single-molecule precision. *Nat. Commun.* **2023**, *14*, 1374.
[240] Fuller, C. W.; Kumar, S.; Porel, M.; Chien, M.; Bibillo, A.; Stranges, P. B.; Dorwart, M.; Tao, C. J.; Li, Z. M.; Guo, W. J. et al. Real-time single-molecule electronic DNA sequencing by synthesis using polymer-tagged nucleotides on a nanopore array. *Proc. Natl. Acad. Sci. USA* **2016**, *113*, 5233–5238.
[241] Stranges, P. B.; Palla, M.; Kalachikov, S.; Nivala, J.; Dorwart, M.; Trans, A.; Kumar, S.; Porel, M.; Chien, M.; Tao, C. J. et al. Design and characterization of a nanopore-coupled polymerase for single-molecule DNA sequencing by synthesis on an electrode array. *Proc. Natl. Acad. Sci. USA* **2016**, *113*, E6749–E6756.
[242] Palla, M.; Punthambaker, S.; Stranges, B.; Vigneault, F.; Nivala, J.; Wiegand, D.; Ayer, A.; Craig, T.; Gremyachinskiy, D.; Franklin, H. et al. Multiplex single-molecule kinetics of nanopore-coupled polymerases. *ACS Nano* **2021**, *15*, 489–502.
[243] Lin, M. S.; Zhang, G.; Fahie, M.; Morgan, L. K.; Chen, M.; Keiderling, T. A.; Kenney, L. J.; Liang, J. Engineering a novel porin OmpGF via strand replacement from computational analysis of sequence motif. *Biochim. Biophys. Acta-Biomembr.* **2017**, *1859*, 1180–1189.
[244] Ho, C. W.; Van Meervelt, V.; Tsai, K. C.; De Temmerman, P. J.; Mast, J.; Maglia, G. Engineering a nanopore with co-chaperonin function. *Sci. Adv.* **2015**, *1*, e1500905.
[245] Van der Verren, S. E.; Van Gerven, N.; Jonckheere, W.; Hambley, R.; Singh, P.; Kilgour, J.; Jordan, M.; Wallace, E. J.; Jayasinghe, L.; Remaut, H. A dual-constriction biological nanopore resolves homonucleotide sequences with high fidelity. *Nat. Biotechnol.* **2020**, *38*, 1415–1420.
[246] Motone, K.; Kontogiorgos-Heintz, D.; Wee, J.; Kurihara, K.; Yang, S.; Roote, G.; Fox, O. E.; Fang, Y. S.; Queen, M.; Tolhurst, M. et al. Multi-pass, single-molecule nanopore reading of long protein strands. *Nature* **2024**, *633*, 662–669.
[247] Su, Z. Q.; Chen, T. T.; Liu, X. T.; Kang, X. F. Size-tunable transmembrane nanopores assembled from decomposable molecular templates. *Biosens. Bioelectron.* **2025**, *267*, 116780.
[248] Sun, K.; Zhao, C. J.; Zeng, X. J.; Chen, Y. J.; Jiang, X.; Ding, X. T.; Gou, L.; Xie, H. Y.; Li, X. Q.; Zhang, X. L. et al. Active DNA unwinding and transport by a membrane-adapted helicase nanopore. *Nat. Commun.* **2019**, *10*, 5083.
[249] Zhao, C. J.; Li, K. J.; Mou, X. Y.; Zhu, Y. B.; Chen, C.; Zhang, M.; Wang, Y.; Zhou, K.; Sheng, Y. Y.; Liu, H. et al. High-fidelity biosensing of dNTPs and nucleic acids by controllable subnanometer channel PaMscS. *Biosens. Bioelectron.* **2022**, *200*, 113894.
[250] Vorobieva, A. A.; White, P.; Liang, B. Y.; Horne, J. E.; Bera, A. K.; Chow, C. M.; Gerben, S.; Marx, S.; Kang, A.; Stiving, A. Q. et al. De novo design of transmembrane β barrels. *Science* **2021**, *371*, eabc8182.
[251] Fujita, S.; Kawamura, I.; Kawano, R. Cell-free expression of *de novo* designed peptides that form β-barrel nanopores. *ACS Nano* **2023**, *17*, 3358–3367.
[252] Cardozo, N.; Zhang, K. R.; Doroschak, K.; Nguyen, A.; Siddiqui, Z.;

Bogard, N.; Strauss, K.; Ceze, L.; Nivala, J. Multiplexed direct detection of barcoded protein reporters on a nanopore array. *Nat. Biotechnol.* **2022**, *40*, 42–46.

[253] Bei, W. W.; Luo, Q. S.; Shi, H. G.; Zhou, H. Z.; Zhou, M.; Zhang, X. Z.; Huang, Y. H. Cryo-EM structures of LolCDE reveal the molecular mechanism of bacterial lipoprotein sorting in *Escherichia coli*. *PLoS Biol.* **2022**, *20*, e3001823.

[254] Pastoriza-Gallego, M.; Rabah, L.; Gibrat, G.; Thiebot, B.; van der Goot, F. G.; Auvray, L.; Betton, J. M.; Pelta, J. Dynamics of unfolded protein transport through an aerolysin pore. *J. Am. Chem. Soc.* **2011**, *133*, 2923–2931.

[255] Oukhaled, G.; Mathé, J.; Biance, A. L.; Bacri, L.; Betton, J. M.; Lairez, D.; Pelta, J.; Auvray, L. Unfolding of proteins and long transient conformations detected by single nanopore recording. *Phys. Rev. Lett.* **2007**, *98*, 158101.

[256] Yu, L. N.; Kang, X. Q.; Li, F. J.; Mehrafrooz, B.; Makhamreh, A.; Fallahi, A.; Foster, J. C.; Aksimentiev, A.; Chen, M.; Wanunu, M. Unidirectional single-file transport of full-length proteins through a nanopore. *Nat. Biotechnol.* **2023**, *41*, 1130–1139.

[257] Teng, H. T.; Cao, M. D.; Hall, M. B.; Duarte, T.; Wang, S.; Coin, L. J. M. Chiron: Translating nanopore raw signal directly into nucleotide sequence using deep learning. *Gigascience* **2018**, *7*, giy037.

[258] Lv, X.; Chen, Z. G.; Lu, Y. T.; Yang, Y. D. An end-to-end Oxford nanopore basecaller using convolution-augmented transformer. In *Proceedings of 2020 IEEE International Conference on Bioinformatics and Biomedicine*, Seoul, Korea (South), **2020**, 337–342.

[259] Song, J. W.; Lin, L. A.; Tang, C.; Chen, C.; Yang, Q. X.; Zhang, D.; Zhao, Y. C.; Wei, H. C.; Linghu, K. P.; Xu, Z. J. et al. DEMINERS enables clinical metagenomics and comparative transcriptomic analysis by increasing throughput and accuracy of nanopore direct RNA sequencing. *Genome Biol.* **2025**, *26*, 76.